Spontaneous and induced false vacuum decay

Matthew Citron

September 2013

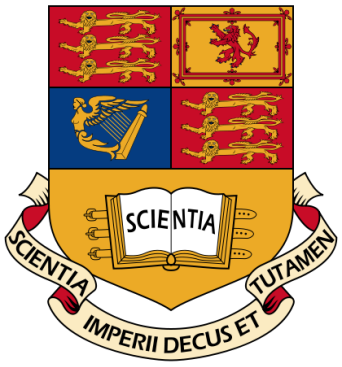

Submitted in partial fulfilment of the requirements for the degree of Master of Science of Imperial College London

Supervised by Dr Arttu Rajantie

IMPERIAL COLLEGE LONDON

MSc

Spontaneous and induced false vacuum decay

by Matthew Citron

Using a semiclassical approximation the probability of spontaneous false vacuum decay in the QM and QFT case is found following the work of Coleman. It is then shown how this is extended such that the suppression exponent for decay via particle collisions can be found. This is translated to a numerically solvable problem on the lattice. Using this, the preliminary results of simulations for spontaneous decays are presented.

Chapter 1

Introduction

1.1 Motivations

1.1.1 Spontaneous vacuum decay

The scalar field can fill many functions in physics. These range from being a candidate for inflation in cosmology [1] to the root of the Higgs effect [2] which explains the mass of the particles in the standard model. Most interesting is the case where its potential exhibits a false minimum. Indeed, the mass found for the Higgs ($\approx 125GeV$) suggests that the effective Higgs potential under the renormalisation group running of its coupling exhibits such a false minimum [3]. The first consideration of what happens if the field is in such a metastable state was carried in the 1970s by Voloshin, Kobzarev, and Okun [4] and developed by Sidney Coleman [5]. Coleman explained the situation using the analogy of free energy in statistical mechanics. Consider a superheated fluid. This has two phases, the liquid (false minimum) phase and the vapour phase. Thermal fluctuations will cause bubbles of vapour to appear. Depending on their initial volume it will be energetically favourable to grow or to shrink. If the bubble is too small it will be destroyed as surface energy decrease compensates volume energy increase. On the other hand, if the volume of the initial bubble is large enough it will grow until the entire system is in the vapour (true minimum) phase. The case for a scalar field is analogous with quantum fluctuations replacing the thermal. As will be shown if a critical bubble of true vacuum forms it will, due to the Lorentz invariance of the problem, immediately begin to expand outwards at the speed of light [6]. This will cause a wall of energy to spread from the point of nucleation consuming everything in its wake, invisible to any observer until it has hit. The probability for such an event per unit volume per unit time is low and so it is a cosmological phenomena. The focus of this project will be on calculating the probability of induced vacuum decay as may be seen in experiment.

Therefore, effects of gravity are neglected. However, it should be mentioned that in cosmology considering gravity along with the effects of bubble nucleation described here allows much to be learnt. For example, this can give hybrid models of inflation which involves "slow-roll" inflation ending with bubble nucleation [7] as well as effects such as cosmic strings [8]. The decay of the false vacuum need not occur spontaneously and it is the focus of this report to consider particle collisions leading to critical bubbles.

1.1.2 Induced vacuum decay

Induced vacuum decay is a highly non-trivial problem and it may be wondered why this problem is relevant – if it were possible for particle collisions at reachable energies on Earth to cause false vacuum decay then spontaneous false vacuum decay in our vicinity would be inevitable. However, this argument neglects the case of degenerate minima. Consider the simplest case of a scalar field in one dimension with a symmetric double well potential. Particle collisions could cause the formation of kink-antikink configurations of false vacuum. This configuration is shown in 1.1 for $V = -1/2\phi^2 + \phi^4$. This potential has degenerate minima at $\phi = \pm 0.5$. In this case the attraction between the kink and the antikink will stop the light speed propagation. This means that there is no destruction of the universe and such an object may be possible to create in, for example, the large hadron collider. It will be shown that such a process forms two widely separated particle like objects. The aim of this project is to find the suppression in the cross-section of the formation of this soliton-antisolition pair. Obviously, we do not live in a 1+1 dimensional world, however, the real interest in the method used is that it may be extended to the case of any topology changing process that can be characterised by an effective potential with a false minimum or symmetric well. This allows the procedure to be extended to objects such as magnetic monopoles. [9].

1.2 Approach used

1.2.1 Overview of method

Perturbation theory is inadequate for such a problem as the bubble formation is a non-perturbative event. To get around this, the semi-classical method developed by Coleman et al is employed. By taking a Wick rotation, it will be shown that for the case of the false minimum, to leading order, the bubble formation may be approximated by considering solutions to the Euclidean field equations. These are the classical field equations for a particle in the negative potential. For induced vacuum decay a partial Wick rotation will be used and it will be shown that the solutions in the tunnelling region will be complex

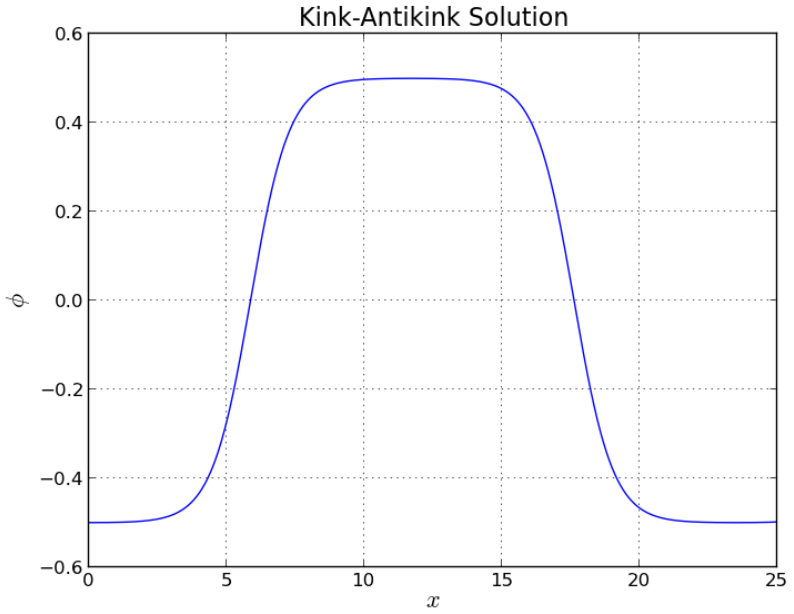

FIGURE 1.1: Kink-Antikink formation. This does not expand at the speed of light due to the lack of pressure from the vacuum

in general. The false vacuum solution must be continued to the limit of degenerate minima for the kink-antikink case.

1.2.2 Organisation of the report

Initially, the simplest case of tunnelling from a false minimum will be considered in Chapter 2 and an expression for the ground state energy and decay time found. The field case in Chapter 3 will then be considered in which it will be shown that most of the results of Chapter 2 may be extended trivially. The effects of bubble nucleation will also be considered. In Chapter 4 the more difficult case of the decay of the false vacuum due to particle collisions will be dealt with. It will be shown that only the suppression exponent may be estimated. In Chapter 5 the previous results will be applied to a lattice to show how they may be simulated. Potential problems in this simulation are also discussed. Finally Chapter 6 contains preliminary results of carrying out simulations for the simplest bounce case in field theory.

Chapter 2

Bounce in quantum mechanics

2.1 Quantum Mechanics

In this section the derivations follow the general strategy from the seminal papers by Sidney Coleman on the fate of the false vacuum [5] and [10]. Starting with the case of a one dimensional particle in a potential well, it is easy to transfer the results to the case of the d dimensional scalar field. So that the effectiveness of the approximation can be proved, it is informative to use instanton methods to re-derive well known results in 1D quantum mechanics. It will be seen that these methods allow exploration of the ground state of the system. First however the general strategy must be outlined. The starting point is Feynman's path integral formulation [11]. To find how a particle evolves from one position to another we can express the expectation value for a particle that starts at x_i at $-t_0/2$ to end at x_f at $t_0/2$ as

$$\langle x_f|\mathrm{e}^{-iHt_0}|x_i\rangle = N\int[\mathrm{D}x]\mathrm{e}^{iS[x(t)]}, \tag{2.1}$$

where $x_{i/f}$ are the initial and final positions, H is the Hamiltonian and $\mathrm{e}^{iS[x(t)]}$ is the evolution operator (S matrix), N is the normalisation and $[\mathrm{D}x]$ is the path element which indicates all possible paths which satisfy the boundary positions are integrated over. The action S is given by

$$S = \int_{-t_0/2}^{t_0/2}\mathrm{d}t\mathcal{L}(x,\dot{x}) = \int_{-t_0/2}^{t_0/2}\frac{1}{2}\left(\frac{\mathrm{d}x}{\mathrm{d}t}\right)^2 - V(x)\mathrm{d}t, \tag{2.2}$$

where $V(x)$ is the potential. The left hand side of the this equation can be expanded in energy eigenstates

$$H|n\rangle = E_n|n\rangle$$

which implies

$$\langle x_f|\mathrm{e}^{-iHt_0}|x_i\rangle = \sum_n \mathrm{e}^{-iE_n t_0}\langle x_f|n\rangle\langle n|x_i\rangle. \tag{2.3}$$

Instanton methods will apply to the ground state of the theory and so the Wick rotation is used. The time is rotated to the complex axis $t \to -i\tau$ and by letting $\tau_0 \to \infty$ all the states with energy higher than E_0 are exponentially suppressed in comparison to the term involving $|0\rangle$. This leaves

$$\mathrm{e}^{-E_0\tau_0}\langle x_f|0\rangle\langle 0|x_i\rangle \equiv \mathrm{e}^{-E_0\tau_0}\psi_0(x_f)\psi_0^*(x_i) \tag{2.4}$$

where $\psi_0(x)$ is the ground state wavefunction at position x. This limit will therefore give the energy and expectation value of the wavefunction of the lowest state. The right-hand side of the action in 2.2 under the Wick rotation takes the form

$$iS[x(t)] \to -S_E = \int_{-\tau_0/2}^{\tau_0/2} -\frac{1}{2}\left(\frac{\mathrm{d}x}{\mathrm{d}\tau}\right)^2 - V(x)\mathrm{d}\tau \tag{2.5}$$

where S_E is the Euclidean action and dependent on the complex part of the time τ. Therefore equation 2.1 becomes

$$\langle x_f|\mathrm{e}^{-H\tau_0}|x_i\rangle = N\int [\mathrm{D}x]\mathrm{e}^{-S_E} \tag{2.6}$$

as $\tau_0 \to \infty$. For the rest of this chapter $S_E \equiv S$ unless otherwise stated. It is obvious that S is positive definite and so the RHS of 2.6 must be exponentially suppressed. If S is large then we expect the solution to be dominated by the minimal path ($\chi(\tau)$). If there are several minima then these must be summed over. This approximation is known as the method of steepest descent [12] (see Appendix A). Denoting the action for this minimal path S_0, 2.6 becomes

$$N\int [\mathrm{D}x]\mathrm{e}^{-S_E} \sim \mathrm{e}^{-S_0}. \tag{2.7}$$

This approximation to the path integral is known as the quasi-classical approximation. The reason for this name can easily be seen by considering which path will minimise the Euclidean action S. The extremal of the functional derivative is given by

$$0 = \delta S = S[\chi(\tau) + \delta x(\tau)] - S[\chi(\tau)] = \int_{-\tau_0/2}^{\tau_0/2} -\frac{\mathrm{d}^2\chi}{\mathrm{d}\tau^2} + V'(\chi)\mathrm{d}\tau, \tag{2.8}$$

so the equation of motion is just

$$\frac{\mathrm{d}^2\chi}{\mathrm{d}\tau^2} = V'(\chi). \tag{2.9}$$

This is just Newton's second law but in a negative potential $-V(x)$. Thus the path which gives the leading contribution to the exponent is that of a classical object feeling the effects of the opposite potential. Immediately using our intuition of classical mechanics it is obvious that the solution must also satisfy energy conservation.

$$E = \frac{1}{2}\frac{\mathrm{d}\chi}{\mathrm{d}\tau}^2 - V = const. \tag{2.10}$$

Later when a complicated initial state is considered only exponential accuracy will be desired. However, for this simple case the prefactor in 2.7 is also calculable. Consider an arbitrary function which solves the boundary conditions. This can be written as

$$x(\tau) = \chi(\tau) + \sum_n c_n x_n(\tau) \tag{2.11}$$

where x_n are orthonormal functions which vanish at the boundaries and so if $\chi(\tau)$ fits the boundary conditions (BC) then so must $x(\tau)$. As the c_n are arbitrary and x_n are orthonormal inside the boundaries any function which satisfies the BC can be written in this form. The measure can then be chosen as

$$[Dx] = \prod_n \frac{\mathrm{d}c_n}{\sqrt{2\pi}}. \tag{2.12}$$

As stated earlier it is assumed that the action is large. This means that its effect will be suppressed away from the minimum. Because of this it is expected that the prefactor will be dependent on the range of paths very near the extremal path [6]. This will keep the action in its relevant regime. Expanding around the minimum gives

$$S[\chi(\tau) + \delta x(\tau)] = \int_{-\tau_0/2}^{\tau_0/2} \frac{1}{2}\left(\frac{\mathrm{d}(\chi + \delta x)}{\mathrm{d}\tau}\right)^2 + V(\chi + \delta x)\mathrm{d}\tau. \tag{2.13}$$

Considering up to quadratic variations (linear variations are negligible by 2.8) and using integration by parts gives

$$S[\chi(\tau) + \delta x(\tau)] = S_0 + \int_{-\tau_0/2}^{\tau_0/2} \delta x \left[-\frac{1}{2}\frac{\mathrm{d}^2\delta x}{\mathrm{d}\tau^2} + \frac{1}{2}V''(\chi)\delta x\right]\mathrm{d}\tau. \tag{2.14}$$

It is then possible to choose the orthonormal functions from 2.11 as the eigenfunctions of the deviations of the action

$$-\frac{1}{2}\frac{\mathrm{d}^2 x_n(\tau)}{\mathrm{d}\tau^2} + \frac{1}{2}V''(\chi)x_n(\tau) \equiv \hat{M}x_n = \epsilon_n x_n(\tau) \tag{2.15}$$

giving

$$S = S_0 + \frac{1}{2}\sum_n \epsilon_n c_n^2 \tag{2.16}$$

Subbing 2.12 and 2.16 into 2.6 and using Gaussian integration finally gives

$$\langle x_f|\mathrm{e}^{-H\tau_0}|x_i\rangle = N\mathrm{e}^{-S_0}\prod_n \epsilon_n^{-1/2} + \text{subleading}, \tag{2.17}$$

where the Gaussian integral,

$$\int \mathrm{d}x\mathrm{e}^{-cx^2} = \frac{\sqrt{2\pi}}{\sqrt{c}}, \tag{2.18}$$

has been used. The eigenvalue product may also be written as

$$\prod_n \epsilon_n^{-1/2} = \left[det\left(-\frac{\mathrm{d}^2}{\mathrm{d}\tau^2} + V''(\chi(\tau))\right)\right]^{-1/2}. \tag{2.19}$$

This can be understood from the finite dimensional matrix case [11]. The normalisation N is fixed depending on the form of the potential desired. In this section the difficult problem of finding the ground state energy and specific expectation values of its wave-function has been reduced to finding a classical solution to the Euclidean field equations. The main subtlety remaining is the calculation of 2.19 which is non-trivial and can be done only for specific potentials. It remains to be seen how this method is applied to finding the decay time of an unstable minimum. Firstly, some well known results are re-derived to show the effectiveness of the procedure.

2.2 Application in well potentials

Ultimately, the aim in this section is to find the time for a particle to tunnel out of a false minimum of a potential. This is equivalent to finding the width of an unstable state. As a starting point, however it is useful to see that we find the expected result when applying the methods discussed above to a simple single well.

2.2.1 Single well

Consider the potential shown in 2.1(a) which has only one minimum. Intuitively, from a classical perspective, we expect that the solution will be periodic and so choose the boundary conditions $x_i = x_f = 0$. Looking at the inverted potential shown in 2.1(b) it's obvious that there is only one solution which can satisfy this

$$\chi(\tau) = 0 \ \forall \ \tau. \tag{2.20}$$

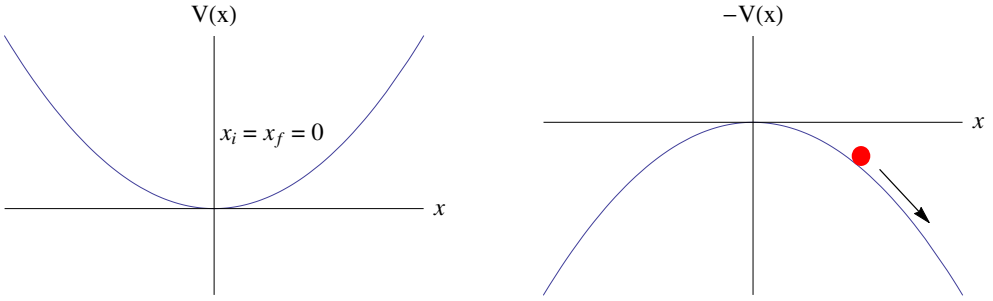

(a) Single well potential (b) Negative potential

FIGURE 2.1: LEFT: An example of a potential that is analysed in this section. Note that this need not be symmetric. RIGHT: Reverse potential with unstable point shown.

If χ takes on any other value, the only possible endpoint to its path will be at positive or negative infinity. The action for this null solution is $S = 0$ meaning

$$\langle 0|\mathrm{e}^{-H\tau_0}|0\rangle = N\left[det\left(-\frac{\mathrm{d}^2}{\mathrm{d}\tau^2}+\omega^2\right)\right]^{-1/2} + \text{subleading}, \tag{2.21}$$

where $\omega = V''(0)$. As the action cannot be negative this must be the minimum of the action. Clearly the eigenfunctions of $\bar{M}$ in this case are just the sin and cos functions which satisfy the condition $x(\pm\tau_0) = 0$ [11]. This fixes the eigenvalues to be

$$\epsilon_n = \frac{\pi^2 n^2}{\tau_0^2} + \omega^2, n = 1, 2, ... \tag{2.22}$$

By splitting the rhs of 2.21 into two factors it is possible to avoid finding N explicitly

$$N\left[det\left(-\frac{\mathrm{d}^2}{\mathrm{d}\tau^2}+\omega^2\right)\right]^{-1/2} = \left[N\prod_{n=1}^{\infty}\left(\frac{\pi^2n^2}{\tau_0^2}\right)^{-1/2}\right]\times\left[\prod_{n=1}^{\infty}\left(1+\frac{\tau_0^2\omega^2}{\pi^2n^2}\right)^{-1/2}\right]. \tag{2.23}$$

The first term has no dependence on ω and so it can be fixed by requiring that it reproduces the free $\omega = 0$ behaviour

$$\left[N\left(\prod_{n=1}^{\infty}\frac{\pi^2n^2}{\tau_0^2}\right)^{-1/2}\right] = \langle 0|\mathrm{e}^{-\hat{p}^2\tau_0/2}|0\rangle = \frac{1}{\sqrt{2\pi\tau_0}}. \tag{2.24}$$

Next, the standard formula [11],

$$\pi y\prod_{n=1}^{\infty}\left(1+\frac{y^2}{n^2}\right) = \sinh(\pi y),$$

may be used to give

$$\langle 0|\mathrm{e}^{-H\tau_0}|0\rangle = \left(\frac{\omega}{\pi}\right)^{1/2}(2\sinh(\omega\tau_0))^{-1/2}. \tag{2.25}$$

Recalling that to arrive at the ground state the limit $\tau \to \infty$ must be taken finally gives

$$\langle 0|\mathrm{e}^{-H\tau_0}|0\rangle \to \left(\frac{\omega}{\pi}\right)^{1/2} \mathrm{e}^{-\omega\tau_0/2}(1+...) \tag{2.26}$$

Comparing this to 2.4 we find, as expected, $E_0 = \omega/2$ and $[\psi_0(0)]^2 = (\omega/\pi)^{1/2}$. This is the result from normal wave mechanics [6]. And so the semiclassical method has returned the correct result for this simple potential. As this result comes from focusing solely on the behaviour very near the minimum, the form of the potential far from this point will not affect the result. Therefore this is the exact result for the harmonic oscillator and an approximation for all other single well potentials. Now that these simple results have been rederived the more complex case of double wells and false minima may be examined.

2.2.2 Double wells and false minima

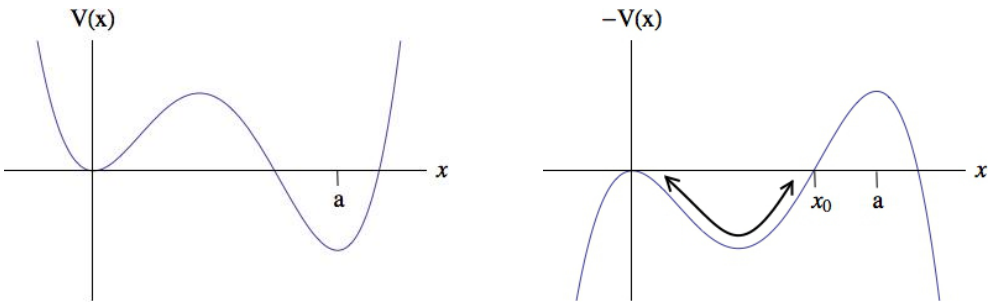

(a) Well potential with local minimum (b) Negative potential

FIGURE 2.2: LEFT: An example of a potential that is analysed in this section. RIGHT: Reverse potential with bounce shown.

Consider a potential of the form in 2.2(a). It has a false minimum at $x = 0$ and a true minima at $x = a$. In the classical case, if a particle were to be trapped in the minimum then apart from external effects (such as thermal excitations), escape would be impossible. In the quantum case however, the phenomena of tunnelling will eventually cause the particle to escape and evolve to the true minimum (or to infinity if such a minimum does not exist). The probability of this occurring is given by the width of the state, which is in turn given by the complex component of the energy. This can be intuitively understood by considering the unitary time evolution operator. The probability of remaining in a state at time t is

$$|\psi(t)|^2 = |U(t)\psi(0)|^2 = \left|\mathrm{e}^{-iEt}\psi(0)\right|^2 = \mathrm{e}^{-\Gamma t}, \tag{2.27}$$

where $\Gamma = -2Im(E)$ is the width of the state and in these units its inverse is the lifetime. Thus the lifetime of an unstable state can be found from the imaginary component of its energy [13].

Some issues are to be expected in finding this lifetime as an unstable state cannot be in the spectrum of the Hamiltonian [10]. Initially, this will be neglected and the solution will naively follow the same method as before until we hit the problem. The potential is inverted and again the classical path is expected to be periodic and so $x_i = x_f = 0$ is taken. Now, however, there are more ways to achieve this than merely the trivial solution. As shown in 2.2(b) the particle may begin on the left at some point just below the height of the local maximum at $x = 0$ and 'bounce' from the potential barrier. As $x = 0$ is approached the time for this bounce to occur must increase. At the end of the problem $\tau_0 \to \infty$ must be taken and this corresponds to the limiting case of the path starting infinitesimally near the maximum and bouncing from the barrier at x_0. This case is known as the instanton solution (from 't Hooft) and has zero total energy. Using conservation of energy will therefore give

$$\frac{dx}{dt} = (2V)^{1/2}. \tag{2.28}$$

At very large times the path must closely approach the point $x_f = 0$ and so here $V(x)$ can be approximated by $1/2\omega^2 x^2$ and 2.28 becomes (choosing the physically relevant negative root)

$$\frac{dx}{dt} = -\omega x, \tag{2.29}$$

but this can be solved to give

$$x \propto \exp -\omega t. \tag{2.30}$$

This implies that the instanton is actually a localised object of size $\approx 1/\omega$. Due to this, they were in fact named "quasi-particles" by Polyakov[14]. The centre of the instanton (where $dx/dt = 0$) is arbitrary by time invariance. This means that instantons are not the only approximate solution to the equations of motion in the $\tau_0 \to \infty$ limit. For $T \gg 1/\omega$ it is possible to have n widely separated bounces, each centred at τ_n such that $-\tau_0/2 < \tau_1 < \tau_2 < ... < \tau_n < \tau_0/2$. To find the solution to 2.6 the sum over all of these configurations must be taken.

The path taken for the bounce is denoted χ and for n bounces we have an action $nS(q_c) \equiv nS_0$. In the vast time separating the bounces the solution will be at $x = 0$, meaning it makes sense to rewrite the problem in terms of the solution to the single well problem (2.26). Consider the leading determinant term for a single bounce,

$$N\left[det\left(-\frac{\mathrm{d}^2}{\mathrm{d}\tau^2} + \omega^2\right)\right]^{-1/2} \times \left\{\frac{det[-\mathrm{d}^2/\mathrm{d}\tau^2 + V''(\chi)]}{det[-\mathrm{d}^2/\mathrm{d}\tau^2 + \omega^2]}\right\}, \tag{2.31}$$

from 2.26 in the infinite τ limit

$$N\left[det\left(-\frac{\mathrm{d}^2}{\mathrm{d}\tau^2}+\omega^2\right)\right]^{-1/2}\rightarrow\left(\frac{\omega}{\pi}\right)^{1/2}\mathrm{e}^{-\omega\tau_0/2} \tag{2.32}$$

and so 2.31 can be written as

$$\left(\frac{\omega}{\pi}\right)^{1/2}\mathrm{e}^{-\omega\tau_0/2}K \tag{2.33}$$

which for n bounces becomes

$$\left(\frac{\omega}{\pi}\right)^{1/2}\mathrm{e}^{-\omega\tau_0/2}K^n. \tag{2.34}$$

The form of K is found by the solution for one bounce [10].

However, there is a problem in finding the determinant. Consider taking a time derivative of the equation of motion 2.9

$$\frac{\mathrm{d}^2}{d\tau^2}\dot{\chi}(\tau)+V''(\chi(t))\dot{\chi}(\tau)=0=\bar{M}\chi. \tag{2.35}$$

So there is a zero mode (denoted x_1) of the operator which gives quadratic deviations from S. As χ is periodic this function also satisfies the BC and it is normalisable [15]. It therefore must be proportional to one of the eigenfunctions of $\hat{M}$. This is a problem because $\epsilon_1 = 0$ implies that the eigenvalue product in 2.17 is divergent. To find the reason for the appearance of the zero mode consider shifting the centre of the bounce. This has no effect on the action and so

$$S[\chi(\tau,\tau_c)]-S[\chi(\tau,\tau_c+\delta\tau)]=0,$$

where $\chi(\tau,\tau_c)$ is the bounce with centre at τ_c. Therefore the zero mode is expected to be that with $\chi(\tau,\tau_c)-\chi(\tau,\tau_c+\delta\tau)=0$ i.e. $\dot{\chi}(\tau)$ [11]. Therefore, the root cause of this zero eigenvalue is time translational invariance. The normalisation of this mode is given by

$$|\dot{\chi}(\tau)|^2=\int_{-\tau_0/2}^{\tau_0/2}\dot{\chi}(\tau)^2\mathrm{d}\tau=S_0,$$

where the last equality follows from energy conservation and the fact that $E = 0$ for the bounc and so the potential gives the same contribution as the kinetic term. By changing variables to χ the bounce action may also be written as

$$S_0=2\int_0^{x_0}\mathrm{d}\chi\sqrt{-2V(\chi)}. \tag{2.36}$$

This means the normalised zero mode is

$$x_1(\tau)=S_0^{-1/2}\frac{\mathrm{d}}{\mathrm{d}\tau}\chi(\tau). \tag{2.37}$$

To remove the divergence the derivation of 2.17 must be retraced.

$$det(\bar{M})^{-1/2} = \prod_n \epsilon_n^{-1/2} = \int \prod_n \frac{\mathrm{d}c_n}{\sqrt{2\pi}} \mathrm{e}^{-1/2\sum_n \epsilon_n c_n^2} = \int \frac{\mathrm{d}c_n}{\sqrt{2\pi}} (det' M)^{-1/2} \tag{2.38}$$

where,

$$det' M = \prod_{n\neq 1} \epsilon_n \tag{2.39}$$

and the term in the integrand involving $\epsilon_1 = 0$ has been factored out. The contribution from $det' M$ is clearly finite and so the divergence must come from the integration over c_1. Using the relationship between c_1 and the position of the centre the source of the infinity can be found. Under a shift Δc_1 using 2.11

$$\Delta x(\tau) = x_1(\tau)\Delta c_1,$$

but the centre of the instanton,τ_c, may also be shifted which from 2.37 and 2.11 gives

$$\Delta x(\tau) = \Delta\chi(\tau, \tau_c) = \frac{\mathrm{d}\chi(\tau,\tau_c)}{\mathrm{d}\tau}\Delta\tau_c = -\sqrt{S_0}x_0(\tau)\Delta\tau_c \tag{2.40}$$

where the negative sign originates from the shift in τ_c being equivalent to a shift in $-\tau$ for χ. This sign is neglected so that the integration limits agree [11]. The result is that $\mathrm{d}c_0 = \sqrt{S_0}\mathrm{d}\tau_c$. This means that the integration over c_1 in 2.38 is equivalent to

$$\int \frac{\mathrm{d}c_n}{\sqrt{2\pi}} = \frac{\sqrt{S_0}}{2\pi}\int_{-\tau_0/2}^{\tau_0/2} \mathrm{d}\tau_c = \frac{\tau_0\sqrt{S_0}}{\sqrt{2\pi}}. \tag{2.41}$$

So the origin of the divergence comes from taking τ_0 to infinity. However, the energy term is that proportional to τ_0 so this is not an issue in its calculation. Inside K^n the integration over the zero mode for each bounce becomes

$$\left(\frac{\sqrt{S_0}}{\sqrt{2\pi}}\right)^n \int_{-\tau_0/2}^{\tau_0/2} \mathrm{d}\tau \int_{-\tau_0/2}^{\tau_1} \mathrm{d}\tau_2 ... \int_{-\tau_0/2}^{\tau_{n-1}} \mathrm{d}\tau_n = \frac{\tau_0^n}{n!}\left(\frac{\sqrt{S_0}}{\sqrt{2\pi}}\right)^n. \tag{2.42}$$

Defining K' to be K with the zero eigenvalue part removed ,the solution to 2.4 is found by summing over the total number of bounces,

$$\sum_{n=0}^{\infty}\left(\frac{\omega}{\pi}\right)^{1/2}\mathrm{e}^{-\omega\tau_0/2}\frac{\left(K'\mathrm{e}^{-S_0}\tau_0\left(\frac{\sqrt{S_0}}{\sqrt{2\pi}}\right)\right)}{n!} = \left(\frac{\omega}{\pi}\right)^{1/2} exp\left(-\omega\tau_0/2 + K'\mathrm{e}^{-S_0}\tau_0\left(\frac{\sqrt{S_0}}{\sqrt{2\pi}}\right)\right). \tag{2.43}$$

Comparing to equation 2.4, this will give a ground state energy of

$$E_0 = (\frac{\omega}{2}\tau_0 - K\mathrm{e}^{-S_0}) + \text{subleading terms}. \tag{2.44}$$

At first it appears that to retain the second term is pointless as it is exponentially suppressed with respect to terms neglected in our calculation. However, this term is in fact the leading contribution to the imaginary part of the energy $Im(E)$[6]. To see this consider again the zero mode. This is an eigenfunction of the Schrödinger operator $\bar{M}$ with zero eigenvalue. However, we must find if this is also the lowest state. There is a theorem which states that for a Schrödinger operator with eigenvalues $\lambda_0 < \lambda_1 < ... < \lambda_k < ...$ the eigenfunction corresponding to λ_k must have exactly k nodes. However, the bounce solution must satisfy $d\chi/dt = 0$ at the midpoint (the point where it bounces from the potential barrier) and so x_1 has a node and is not the eigenfunction of lowest eigenvalue. This means there must exist an eigenfunction x_0 of eigenvalue $\epsilon_0 < 0$ [16]. Therefore, the integral over c_0 will diverge and the noxious effect of treating an unstable state as if it could be in the spectrum of the Hamiltonian has become apparent.

The only way to properly define such a state is through analytical continuation. This is done in [10] and the result is just that K picks up a factor of a half. This means that K is purely imaginary and

$$Im(K) = \frac{1}{2}\frac{S_0}{2\pi}^{1/2} \left|\frac{det'[-\mathrm{d}/\mathrm{d}\tau + V''(\chi)}{det[-\mathrm{d}^2/\mathrm{d}\tau^2 + \omega^2}\right|^{-1/2} + \text{subleading.} \tag{2.45}$$

Finally the width of the state (reinserting $\hbar$)

$$\Gamma = -2ImE_0/\hbar = \frac{S_0}{2\pi\hbar}^{1/2} \mathrm{e}^{-S_0/\hbar} \left|\frac{det'[-\mathrm{d}^2/\mathrm{d}\tau^2 + V''(\chi)]}{det[-\mathrm{d}^2/\mathrm{d}\tau^2 + \omega^2]}\right|^{-1/2} \times [1 + O(\hbar)] \tag{2.46}$$

The difference between this case and the single well is that the single well $x(\tau) = 0$ solution has no negative mode and thus the contribution to the imaginary part of the energy is null. Calculating the functional determinants is possible for specific types of potentials in quantum mechanics [11]. Doing this one can show that this equation agrees with the result from standard methods. However, the usefulness of this expression is that it can quickly be extended to scalar field theory which will be the topic of the next section. For completeness the symmetric double well is considered in Appendix C. In this case there is no longer an unstable state and so the true ground state of the Hamiltonian may be found. There are two states corresponding to an even or odd superposition of the wavefunction of the particle in the two degenerate minima. These states have energies given by

$$E_\pm = \frac{1}{2}\omega \pm K\mathrm{e}^{-S_0} \tag{2.47}$$

The wavefunction is therefore "smeared" by tunneling. It is remarkable that this effect has sprung from considering classical solutions in the inverse potential. A final comment must be made on the validity of the approach in both cases. The assumption of having

n widely separated bounces is known as the instanton gas approximation. To be trustworthy the instantons must be widely separated in comparison to their size. Consider the sum in 2.43. This is of the form

$$\sum \frac{x^n}{n!}$$

such a sum is determined by the terms such that $x \simeq n$ as higher powers will be increasingly suppressed. This means that the important terms are those such that $n \lesssim K\tau_0 \mathrm{e}^{-S_0}$. The condition for convergence is that n/T is small. Assume S_0 contains a coupling constant λ. Reinserting $\hbar$ and scaling such that $S_0 = 1/\hbar\lambda\tilde{S}_0$ shows that the condition for convergence is clearly $\hbar\lambda \ll 1$.

Chapter 3

Bounce in scalar QFT

3.1 Bubble creation

Much of the results from Chapter 2 can be simply transferred to the multidimensional scalar field. In this section a potential which again has a false minimum is considered. This is now the false vacuum for the scalar field. In d dimensions the action is given by

$$S(\phi) = \int \mathrm{d}^d x \left(\frac{1}{2} (\partial_\mu \phi)^2 + U(\phi) \right). \tag{3.1}$$

Again the potential is assumed to have two minima – a false vacuum at ϕ_+ and a true minimum at ϕ_-. The potential is offset such that $U(\phi_+) = 0$. This means that $\phi = \phi_+$ is equivalent to $x = 0$ in the previous potential. Two main sources of difference between this and the one dimensional QM case are expected: the effect of $d > 1$ and the need to renormalise the action. The steps that led to the end result for the QM case will be followed until these issues present themselves. The problem we wish to solve is the generalisation of 2.1 to d dimensions where position is replaced with field configuration.

$$\langle \phi_f | \mathrm{e}^{-iHt_0} | \phi_i \rangle = N \int [\mathrm{D}\phi] \mathrm{e}^{iS[\phi(\vec{x},t)]} \tag{3.2}$$

The starting point of the Wick rotation and taking $\tau_0 \to \infty$ is unchanged. The Euclidean action for the scalar field is

$$S_E = \int \mathrm{d}^d x \left(\frac{1}{2} (\nabla \phi)^2 + \frac{1}{2} (\frac{\mathrm{d}}{\mathrm{d}\tau} \phi)^2 + U(\phi) \right) \tag{3.3}$$

where the time integration is over τ. For the rest of this chapter again $S \equiv S_E$. This action leads to the Euclidean equation of motion

$$\nabla^2\phi + \frac{\mathrm{d}^2}{\mathrm{d}\tau^2}\phi = U'(\phi). \tag{3.4}$$

The problem under consideration is the instability of the false vacuum and so it makes sense to again look at the case where the solution starts and ends at $\phi = \phi_+$. This implies the boundary condition

$$\phi(\vec{x}, \tau) \to \phi_+, \quad \tau \to \pm\infty. \tag{3.5}$$

As the bounce action must be finite and the integrand is only zero at $\phi = \phi_+$, this gives the large $\vec{x}$ boundary conditions

$$\phi(\vec{x}, \tau) \to \phi_+, \quad |\vec{x}| \to \infty \tag{3.6}$$

and so ϕ returns to the false vacuum value at large spatial distances. This configuration is known as the "critical bubble" as ϕ will be at its false vacuum value everywhere except from a small region around the zero – a critical bubble of true vacuum. The critical bubble solution will be denoted ϕ_c. In [17] Coleman et al have shown that there is exactly one negative mode. This is as required for the solution to have complex energy and thus correspond to an unstable state. The operator corresponding to quadratic deviations from the minimum

$$\bar{M} = -\frac{\mathrm{d}^2}{\mathrm{d}\tau^2} - \nabla^2 + V''(\chi) \tag{3.7}$$

must therefore satisfy

$$det\bar{M} < 0 \tag{3.8}$$

which is easily recognised from the generalisation of 2.15. To proceed, however, first the zero modes have to be properly dealt with. Taking a derivative of 3.4 at ϕ_c with respect to ∂_μ implies $\bar{M}\partial_\mu\phi_c = 0$ and there are now d zero modes. These correspond to the invariance of the bounce under translation in each of the d dimensions. To find the normalisation consider rescaling the dependence of the field by an arbitrary number λ in the action

$$S(\phi_c, \lambda) \equiv S(\phi_c(\lambda x)) = \int \mathrm{d}^d x \frac{1}{2}(\partial_\mu\phi_c(\lambda x))^2 + U(\phi(\lambda x)). \tag{3.9}$$

Changing variables $x \to \lambda x$ gives

$$S(\phi_c, \lambda) = \lambda^{2-d} \int \mathrm{d}^d x \frac{1}{2}(\partial_\mu\phi_c(x))^2 + \lambda^{-d} \int \mathrm{d}^d x U(\phi_c(x)) \tag{3.10}$$

As $\phi_c(\lambda x)$ will satisfy 3.4 for any λ, the action must be invariant under λ. Using this it is possible to define

$$\frac{\mathrm{d}S(\phi_c,\lambda)}{\mathrm{d}\lambda}|_{\lambda=1} = (2-d)\int \mathrm{d}^d x \frac{1}{2}(\partial_\mu \phi_c(x))^2 - d\int \mathrm{d}^d x U(\phi_c(x)) = 0. \tag{3.11}$$

Rearranging this expression to find the integral of $U(\phi_c(x))$ in terms of the integral of the derivative allows the action to be rewritten

$$S_c = S(\phi_c(\lambda x)) = \frac{1}{d}\int \mathrm{d}^d x (\partial_\mu \phi_c(x))^2. \tag{3.12}$$

The orthogonality of the zero modes implies that the zero modes $\phi_\mu = \partial_\mu \phi_c$ have a norm given by

$$\int \mathrm{d}^d x \phi_\mu \phi_\nu = \frac{1}{d}\delta_{\mu\nu} int \mathrm{d}^d x (\partial_\mu \phi_c(x))^2 = \delta_{\mu\nu} S_c \tag{3.13}$$

As expected, the action S_c must be positive definite by 3.12. This means the eventual exponent dependence of the energy will be purely negative, as expected. Comparing to the QM case, the zero mode coefficient c_1 is replaced by $c_\mu^{(1)}$. Then equation 2.38 becomes, to leading order in coupling constant,

$$det(\bar{M})^{-1/2} = \prod_\mu^d \prod_n (\epsilon_\mu^n)^{-1/2} = \int \prod_{\mu=1}^d \prod_n \frac{\mathrm{d}c_\mu^n}{\sqrt{2\pi}} \mathrm{e}^{-1/2\sum_n \epsilon_n c_n^2} = (\int \prod_{\mu=1}^d \frac{\mathrm{d}c_\mu^1}{\sqrt{2\pi}})(det' M)^{-1/2}. \tag{3.14}$$

Analogously to the QM case the integral over the zero modes becomes

$$\frac{1}{(2\pi)^{d/2}}\int \prod_{\mu=1}^d \mathrm{d}c_\mu^1 = \frac{S_c^{d/2}}{(2\pi)^{d/2}}\int \prod_{\mu=1}^d \mathrm{d}x_\mu = \frac{S_c^{d/2} V \tau_0}{(2\pi)^{d/2}}, \tag{3.15}$$

where V is the volume of $d-1$ space and τ_0 is the total time. The relevant parameter is now the decay rate per unit volume and so this factor of V has naturally appeared. This is the expected relevant quantity for a field theory. The next step is to find the actual form of the bounce.

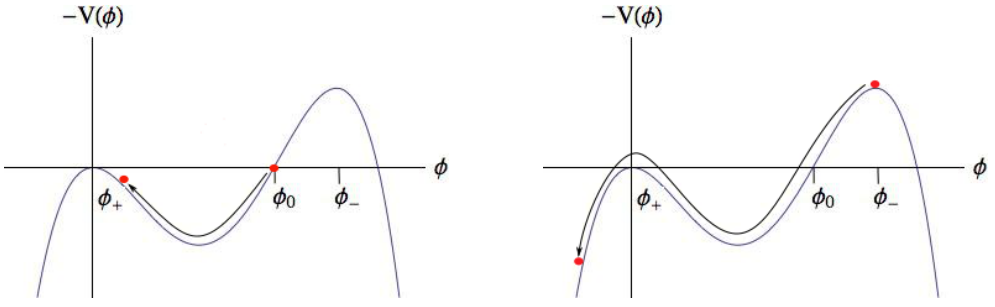

(a) Well Potential Showing Undershoot (b) Well Potential Showing Overshoot

FIGURE 3.1: Reverse of potential. The method of overshoot/undershoot is shown.

Finding the bounce is simplified by the proof by Coleman et al. that the configuration which minimises the action must always be $O(4)$ symmetric [17]. This means that the solution $\phi_c(\vec{x}, \tau)$ can be written as $\phi(r)$ where $r = \sqrt{\vec{x}^2 + \tau^2}$. The equation of motion 3.4 can be transformed to

$$\frac{\mathrm{d}^2\phi_c}{\mathrm{d}r^2} + \frac{d-1}{r}\frac{\mathrm{d}\phi_c}{\mathrm{d}r} = U'(\phi_c) \tag{3.16}$$

and the boundary conditions become

$$\lim_{r\to\infty} \phi_c = \phi_+, \tag{3.17}$$

while to keep the problem well defined at the origin

$$\frac{\mathrm{d}\phi_c}{\mathrm{d}r}|_{r=0} = 0. \tag{3.18}$$

To understand this equation consider ϕ as the position of a particle with time characterised by r. In this scenario, 3.16 describes a particle moving in a potential of $-U$ with a time dependent damping term inversely proportional to the mass. It can be seen that this reduces to the QM case (no damping) for $d = 1$ as expected. Considering figure 3.1 it can be seen that the bounce is the solution which starts on the potential barrier and moves towards ϕ_+ such that it reaches its end point as $r \to \infty$. Unlike the $d = 1$ case the starting point will not be at $U(\phi_0) = 0$ due to the damping term. The existence of such a solution will now be demonstrated using an undershoot-overshoot argument.

Consider releasing the particle to the left of ϕ_0 (figure 3.1(a)) the particle will not have sufficient energy to climb the hill and will therefore never reach the false vacuum (the damping term will only act to reduce the energy available). Thus the particle will undershoot. Now consider releasing the particle very near to ϕ_- (figure 3.1(b)). It can be shown that it is possible to remain as near as desired to ϕ_- for arbitrary r. But looking at 3.16 the damping term is inversely proportional to r and can be neglected as $r \to \infty$. This means the particle overshoots and by continuity there must exist a solution such that the particle comes to rest at ϕ_+. Putting everything together, the solution to leading order in coupling constant is

$$\Gamma/V = -2ImE/V = \frac{1}{2}\frac{S_c^{d/2}\beta}{\sqrt{(2\pi)^{d/2}}}\left|\frac{det'[-\mathrm{d}^2/\mathrm{d}\tau^2 - \nabla^2 + U''(\phi_c)}{det[-\mathrm{d}^2/\mathrm{d}\tau^2 - \nabla^2 + U''(\phi_+)}\right|^{-1/2}\mathrm{e}^{-S_c} \tag{3.19}$$

This is the final result for a non-renormalised theory. The most important aspect for a numerical study is the fact that the suppression exponent is just the action of the bounce. To deal with renormalisation only requires a simple extension. Consider the method of minimal subtraction where the action is rewritten in terms of renormalised

quantities and divergences are subtracted by adding counter-terms. This gives (keeping $\hbar$)

$$S = S_R + \sum_{n=1}^{\infty} \hbar^n S^{(n)} \tag{3.20}$$

where $S^{(n)}$ includes all counter terms at n loops. The bounce is computed for S_R. To ensure that the minimum of the action is at zero as required for the convention chosen it is necessary to offset S_c as $S_c \to S_c - S(\phi_+)$. Expanding to first order shows that only one loop corrections are required and

$$\begin{aligned} S(\phi) &= S_R(\phi_c + \hbar\phi^{(1)} + ...) + \hbar S^{(1)}(\phi_c + \hbar\phi^{(1)} + ...) + ... \\ &= S_R(\phi_c) + \hbar S^{(1)}(\phi_c) + ... \end{aligned} \tag{3.21}$$

This implies finally that for a renormalised theory

$$\begin{aligned} \Gamma/V &= \frac{1}{2}\frac{S_c^{d/2}\beta}{\sqrt{(2\pi)^{d/2}}}\left|\frac{det'[-\mathrm{d}^2/\mathrm{d}\tau^2 - \nabla^2 + U''(\phi_c)}{det[-\mathrm{d}^2/\mathrm{d}\tau^2 - \nabla^2 + U''(\phi_+)}\right|^{-1/2} \mathrm{e}^{-S_c + S(\phi_+)} \\ &\simeq \frac{1}{2}\frac{S_R(\phi_c)^{d/2}\beta}{\sqrt{(2\pi)^{d/2}}}\left|\frac{det'[-\mathrm{d}^2/\mathrm{d}\tau^2 - \nabla^2 + U''(\phi_c)}{det[-\mathrm{d}^2/\mathrm{d}\tau^2 - \nabla^2 + U''(\phi_+)}\right|^{-1/2} \mathrm{e}^{-S_R(\phi_c) - \hbar S^{(1)}(\phi_c) + S^{(1)}(\phi_+)} \end{aligned} \tag{3.22}$$

This expression is completely free of ultraviolet divergences for any renormalisable potential. It is useful to see that the result can be renormalised in principle; however, this will not change the form of the solution and so in the remainder of this report the renormalisation will not be carried out.

3.2 Thin wall limit

While 3.16 is usually non-solvable without numerical methods there is a special case where the form of the bounce configuration can be found analytically. In this scenario an approximate solution of 3.16 can be found. The potential considered is an even function of ϕ ($U_+(\phi)$) with minima at $\phi_\pm = \pm$a which is perturbed so that one minima is slightly above the other

$$U = U_+ + \epsilon(\phi - a)/2a \tag{3.23}$$

where $\epsilon > 0$ so that the false minima ϕ_+ is ϵ above ϕ_-. Choosing $\phi(0)$ very near ϕ_- the particle must stay very close to this maximum until a time R has passed. If R is very large then the damping term may be neglected in 3.16 (exactly how large R is determines the validity of the approximation – see below). This means that the bounce will look like a large bubble of true vacuum with radius R with a thin wall where ϕ transitions to its false vacuum value. The term involving ϵ is assumed to be small and

is neglected. Under this approximation 3.16 becomes

$$\frac{\mathrm{d}^2}{\mathrm{d}r^2}\phi_c = U'_+(\phi_c). \tag{3.24}$$

Which is exactly the same equation as evaluated for the bounce in the QM case. The solution desired is therefore a one dimensional instanton which transitions from $-a$ to a as r increases through R. The value of the bubble radius may also be found. As an example the physically relevant case $d = 4$ is assumed. The value of the action is

$$S = 2\pi^2 \int_0^\infty \mathrm{d}r r^3 \left(\frac{1}{2} \frac{\mathrm{d}\phi_c}{\mathrm{d}r}^2 + U \right) \tag{3.25}$$

Dividing this integral into three regions – outside, wall and inside – there are three seperate contributions. On the outside $\phi = \phi_+$ and $U(\phi_+) = 0$ so this gives no contribution. For the inside the derivative contribution is similarly trivially zero as $\phi = \phi_-$, however in this case $U(\phi_-) = -\epsilon$ and there is a contribution of

$$-\frac{1}{2}\pi\epsilon R^4.$$

For the wall contribution the assumption is that the wall is thin and so $r \simeq R$. Using the fact that ϵ dependent terms in U will be negligible in this small region

$$2\pi^2 R^3 \int_0^\infty \mathrm{d}r \left(\frac{1}{2} \frac{\mathrm{d}\phi_c}{\mathrm{d}r}^2 + U_+ \right) = 2\pi^2 R^3 \int_0^\infty \mathrm{d}r (2U_+) \tag{3.26}$$

where energy conservation has been used along with the fact that the instanton solution has $E = 0$ means

$$\frac{1}{2} \frac{\mathrm{d}\phi_c}{\mathrm{d}r}^2 = U_+.$$

By changing variables to ϕ finally gives the wall contribution as

$$2\pi^2 R^3 \int_{-a}^{a} (2U_+)^{1/2} \mathrm{d}\phi = 2\pi^2 R^3 S_1. \tag{3.27}$$

Now R can be found by using the fact that the action is R independent

$$\frac{\mathrm{d}S}{\mathrm{d}R} = 0 = -2\pi^2 R^3 \epsilon + 6\pi^2 R^2 S_1 = 0 \to R = \frac{3S_1}{\epsilon}. \tag{3.28}$$

The action of the bounce is then given as

$$S_c = \frac{27\pi^2 S_1^4}{2\epsilon^3} \tag{3.29}$$

Recalling that in the QM case the instantons were localised objects of size of order $1/\omega$ where $\omega^2 \equiv U''(x_+)$ this suggests that the size of the bounce in this case is approximately

μ where $\mu^2 \equiv U''(\phi_+)$. The validity of this approximation is in the region $R\mu \gg 1$ or equivalently

$$3S_1\mu \gg \epsilon. \tag{3.30}$$

3.3 Fate of the false vacuum

First consider what happens when a particle tunnels from the false minimum in QM. After the quantum tunnelling is over it arrives at the point where the potential energy is zero with zero kinetic energy. It then propagates classically in the potential with these starting conditions. The case for the scalar field is analogous. The point where all velocities are zero is the midpoint of the bounce and so at the end of the quantum evolution (taken at $\tau = 0$) it should arrive at the state defined by

$$\begin{aligned} \phi(t=0,\vec{x}) &= \phi_c(\tau=0,\vec{x}) \\ \partial_t\phi(t=0,\vec{x}) &= 0 \end{aligned} \tag{3.31}$$

and then propagate with the classical field equation

$$\partial_\mu\partial^\mu\phi = U'(\phi). \tag{3.32}$$

This implies that the shape of the bounce in Euclidean space should define the shape of the bubble at the moment of its creation. To see that the bounce satisfies the second condition consider

$$\partial_t\phi = \frac{\mathrm{d}\phi_c}{\mathrm{d}r}\partial_t r = -\frac{t}{r}\frac{\mathrm{d}\phi_c}{\mathrm{d}r} \tag{3.33}$$

which is clearly zero at t = 0. As 3.32 is just the analytical continuation of the Euclidean field equation this implies the solution after the bubble materialises is just the analytical continuation of the bounce

$$\phi(t,\vec{x}) = \phi_c(\rho = (|\vec{x}|^2 - t^2)^{1/2}). \tag{3.34}$$

This has important consequences for the bubble solution. The first is that the $O(4)$ symmetry satisfied by the bounce must turn into an $O(3,1)$ symmetry (Lorentz invariance) after the quantum propagation. It is informative here to consider the solvable thin wall limit. There is a localised wall at the position $\rho = R$ at $t = 0$. Lorentz invariance demands that the future propagation of the position of this wall must satisfy

$$|\vec{x}|^2 - t^2 = R^2. \tag{3.35}$$

This means after its creation the bubble will expand at approximately the speed of light. Indeed when an observer is by the wall then after $R = \mathcal{O}(10^{-21})$ they will be on the inside. This means that if there happen to be any bubbles expanding towards us they would be unobservable until the instant they hit. What effect this would have on a particle (or a human) depends on the reaction of the particles to this wall. Some idea can be gleaned from the amount of energy it carries. The energy of the wall per unit area at zero velocity is given approximately by the Euclidean instanton action S_1. By the Lorentz invariance a section of wall with expansion speed v must carry energy $S_1(1-v)^{-1/2}$ per unit area. For a time when the radius of the bubble is at $|\vec{x}|$ and using

$$v = \frac{\mathrm{d}}{\mathrm{d}t}|\vec{x}| = \frac{(|\vec{x}|^2 - R^2)^{1/2}}{|\vec{x}|} \tag{3.36}$$

the energy of the bubble will be

$$E_{wall} = 4\pi\frac{|\vec{x}|^3 S_1}{R} = 4\pi\frac{|\vec{x}|^3\epsilon}{3} \tag{3.37}$$

In this chapter an equation for the rate of spontaneous false vacuum decay has been derived. The remnants of such a decay would have cosmological consequences and would leave signatures on the cosmic microwave background which do not seem to be present [18]. This leaves the roll of bubble nucleation as the starting point of inflation in doubt. It could be that the barrier is too high or that the vacuum of the universe is stable. In either case there is another way for bubbles of true vacua to occur that may be relevant in high energy physics. Particle collisions may cause the formation of a critical bubble of true vacuum. The cross-section of this is the focus of the next chapter.

Chapter 4

Vacuum decay from particle collisions

In this chapter the aim is to find a way of approximating the cross-section of bubble formation from particle collisions. Such a problem is highly non-trivial and will not give an analytical solution. Indeed, using a semi-classical approximation may only give an approximation of the exponential suppression of the process. This is useful in, for example, determining whether such a process has any possibility of being observed at the Large Hadron Collider (LHC). In this section instead of the infinite periodic instantons of Chapter 3 the focus will shift to complex solutions of the Euclidean field equations with non-infinite period. In [19] they are shown to be a useful tool in finding a semi-classical approximation of the cross section of false vacuum decay from multi particle cross-section at energy E. If the likelihood of, for example, observing such a bubble in the Large Hadron Collider (LHC) is desired then the number of particles in the collision must be fixable. Two-particle collisions will form the vast majority of such processes and in [20] and [21] it was shown that the approach of [19] can be used to find the exponential dependence of this cross section. This derivation is followed in the following section.

4.1 RST formalism

The final cross-section that will be the outcome of this analysis is denoted $\sigma_2(E)$. At first glance it may seem futile to try to use a semi-classical method similar to the bounce to derive the effects of particle collisions on the false vacuum. The process of two particles $\rightarrow$ vacuum bubble has a simple final state amenable to the methods of Chapter 3. However, this process is exclusive due to the two particle initial state and

so cannot be accurately described semiclassically. To get around this, instead of looking at such a state directly it is assumed that a small alteration of this state will not effect the outcome exponentially. Therefore, it should be possible to find a semiclassical state which gives a final cross-section of false vacuum decay near to that of the two particle state [21]. Consider

$$\sigma_N(E) = \sum_{f,i} |\langle f|\hat{S}\hat{P}_E\hat{P}_N|i\rangle|^2. \tag{4.1}$$

where all initial and final states are summed over, $\hat{S}$ is the S-matrix, $\hat{P}_E$ is the projection onto constant energy E and $\hat{P}_N$ is the projection onto constant particle number N. If N is large then this quantity can be calculated semiclassically [22]. The first thing to be noted is that this quantity must provide an upper bound on $\sigma_2(E)$. As the sum is over all initial states one of these must involve $N-2$ free particles and 2 colliding particles and so

$$\sigma_N(E) > \sigma_2(E). \tag{4.2}$$

A lower bound may also be found using the modified projection approach [23]. Assume there is a state $|\psi_N\rangle$ that saturates the sum in 4.1. If the process of two particles to any final state occurs via some intermediate state then substituting $|\psi_N\rangle$ for this state will decrease the cross-section. Consider starting in state $|2\rangle$. As the cross-section sum is dominated by $|\psi_N\rangle$ one must find the overlap of $|2\rangle$ with $|\psi_N\rangle$. However as this will neglect the preferred intermediate state, this will give the inequality

$$|\langle\psi_N|2\rangle|^2\sigma_N(E) < \sigma_2(E) \tag{4.3}$$

and by substituting $|\langle\psi_N|2\rangle|^2 \approx exp(-\text{const}N)$,

$$exp(-\text{const}N)\sigma_N(E) < \sigma_2(E) < \sigma_N(E). \tag{4.4}$$

This means that σ_N must be approximately equal (when 4.4 holds) to σ_2 in the limit $N \to 0$. However, it is possible to go further. The last step requires the coupling constant of the scalar theory. Denoting it by λ, the energy and particle number may be written as

$$\begin{aligned} E &= \frac{\epsilon}{\lambda} \\ N &= \frac{\nu}{\lambda}. \end{aligned} \tag{4.5}$$

It will be shown in the following section that the cross-section can be written as

$$\sigma_N(E) = exp\left[\frac{1}{\lambda}F(\epsilon,\nu) + \mathcal{O}(\lambda^0)\right] \tag{4.6}$$

where F will be determined by the classical solution to the equations of motion. This holds in the limit where $\lambda \to 0$ with fixed ϵ and ν. Using 4.4 in this limit it can be seen

that

$$\lim_{\lambda\to 0} \lambda \ln \sigma_2(E) = F(\epsilon,\nu) + \mathcal{O}(\nu). \tag{4.7}$$

Therefore the exponential part of $\sigma_2(E)$ is determined by calculating $F(\epsilon,\nu)$ in the limit $\nu \to 0$. In the case where a smooth limit cannot be taken this implies that the assumptions leading to 4.3 are false. In this case the other inequality will still hold and $\sigma_N(E)$ will provide an upper limit to $\sigma_2(E)$. In other words if $\sigma_N(E)$ is exponentially suppressed then $\sigma_2(E)$ must be also. Some perturbative work has been done to show when this limit can be taken [21].

4.2 Setting up the problem

This derivation follows that in [21] and reviewed in [22]. Consider a theory with one scalar field $\phi(x)$. In this section the coherent state formalism is used (see Appendix A)[1]. In field space the coherent state can be written as

$$\langle\phi|a\rangle = N.exp\left[-\frac{1}{2}\int \mathrm{d}k a_k a_{-k} - \frac{1}{2}\int \mathrm{d}k \omega_k \phi(\mathbf{k})\phi(-\mathbf{k}) + \int \mathrm{d}k \sqrt{2\omega_k} a_k \phi(\mathbf{k})\right], \tag{4.8}$$

where

$$\frac{1}{(2\pi)^{d/2}}\int \mathrm{d}^d x e^{i\mathbf{k}.\mathbf{x}}\phi(x) \equiv \phi(\mathbf{k}). \tag{4.9}$$

Now 4.1 must be converted into a coherent space expression. In this space operators are represented by their kernel $S(b^*,a) \equiv \langle b|\hat{S}|a\rangle$. Using the completeness relation for ϕ, $S(b^*,a)$ can be written as

$$S(b^*,a) = \int \mathcal{D}\phi_i(\mathbf{x})\mathcal{D}\phi_f(\mathbf{x})\langle b|\phi_f\rangle\langle\phi_f\rangle\phi_f|\hat{S}|\phi_i\rangle\langle\phi_i|a\rangle, \tag{4.10}$$

where ϕ_i and ϕ_f are the initial and final values of $\phi(\mathbf{x})$ respectively. The projection operators must also be written in this form. $\hat{P}_E$ is given by [24]

$$\langle b|\hat{P}_E|a\rangle = \int \mathrm{d}\xi \langle b|\mathrm{e}^{i\bar{H}_0\xi - E\xi}|a\rangle = \int \mathrm{d}\xi exp\left[-iE\xi + \int \mathrm{d}^3k b_k^* a_k \mathrm{e}^{i\omega_k\xi}\right], \tag{4.11}$$

where $\bar{H}_0$ is the free Hamiltonian. The last equality follows using the overlap between coherent states A.12:

$$\langle b|\mathrm{e}^{i\bar{H}_0\xi}|a\rangle = \langle\{b_k\}|\{a_k\mathrm{e}^{i\omega_k\xi}\}\rangle = \int \mathrm{d}\mathbf{k} b_k^* a_k \mathrm{e}^{i\omega_k\xi} \tag{4.12}$$

[1] In this section the coherent states for field theory are denoted by $|a\rangle$ instead of $|\{a_k\}\rangle$ except where this form makes the derivation more explicit

P_N may be found similarly giving

$$\begin{aligned}\langle b|\hat{P}_N|a\rangle &= \int \mathrm{d}\eta exp\left[-iE\eta + \int \mathrm{d}\mathbf{k} b_k^* a_k \mathrm{e}^{i\eta}\right], \\ \langle b|\hat{P}_E|a\rangle &= \int \mathrm{d}\xi exp\left[-iE\xi + \int \mathrm{d}^3k b_k^* a_k \mathrm{e}^{i\omega_k \xi}\right].\end{aligned} \tag{4.13}$$

The time dependence is then removed from the annihilation and creation operators using $a_k \to a_k \mathrm{e}^{-i\omega_k T_i}$ and $b_k^* \to b_k^* \mathrm{e}^{i\omega_k T_f}$. Using this 4.10 may be rewritten as the functional integral (combining initial, final and all interpolating paths of ϕ)

$$S(b^*, a) = \int \mathcal{D}\phi(x) exp\left[iS[\phi] + B_i(\phi_i, a) + B_f(\phi_f, b^*)\right]. \tag{4.14}$$

The boundary terms are given by

$$B_i(\phi_i, a) = \int \mathrm{d}^3k - \frac{1}{2}a_k a_{-k}\mathrm{e}^{-2i\omega_k T_i} - \frac{1}{2}\omega_k \phi_i(\mathbf{k})\phi_i(-\mathbf{k}) + \sqrt{2\omega_k} a_k \mathrm{e}^{-i\omega_k T_i}\phi_i(\mathbf{k}) \tag{4.15}$$

$$B_f(\phi_f, b^*) = \int \mathrm{d}^3k - \frac{1}{2}b_k^* b_{-k}^*\mathrm{e}^{-2i\omega_k T_f} - \frac{1}{2}\omega_k \phi_f(\mathbf{k})\phi_f(-\mathbf{k}) + \sqrt{2\omega_k} b_k^* \mathrm{e}^{-i\omega_k T_f}\phi_f(\mathbf{k}) \tag{4.16}$$

To complete the transformation to coherent state representation firstly the sums are replaced by

$$\begin{aligned}\sum_i &\to \int \mathcal{D}a_k^* \mathcal{D}a_k exp\left[-\int \mathrm{d}^3k a_k^* a_k\right], \\ \sum_f &\to \int \mathcal{D}b_k^* \mathcal{D}b_k exp\left[-\int \mathrm{d}^3k b_k^* b_k\right].\end{aligned} \tag{4.17}$$

Using the completeness relation A.8 generalised to the scalar field case

$$\int \mathcal{D}c_k^* \mathcal{D}c_k exp\left[-\int \mathrm{d}^3k c_k^* c_k\right] |c\rangle\langle c| = 1 \tag{4.18}$$

gives the coherent state form of the cross-section

$$\sigma_N(E) = \int \mathcal{D}[a,b,c,e] exp(-bb^* - aa^* - cc^* - ee^*) S(b^*, c) S(b^*, e) * \langle c|\hat{P}_E\hat{P}_N|a\rangle\langle a|\hat{P}_E\hat{P}_N|e\rangle \tag{4.19}$$

where integrations over momenta are implied and this is a functional integral over all of a, b, c, e. Using 4.13 gives

$$\langle b|\hat{P}_E\hat{P}_N|a\rangle = \int \mathrm{d}\xi \mathrm{d}\eta exp\left[-iE\xi - iN\eta + \int \mathrm{d}^3k \mathrm{e}^{i\omega_k\xi + i\eta} b_k^* a_k\right]. \tag{4.20}$$

Now as many trivial integrations as possible will be carried out to reduce the cross-section to the form of 4.6. To achieve this one may substitute the expressions 4.14 and

4.20 into 4.19 and change variables to remove the exponent term from 4.20 such that $a \to exp(-i\omega\xi - i\eta)a$ and $a^* \to exp(-i\omega\xi' - i\eta')a^*$. This leaves the term involving c_k as

$$\int \mathcal{D}c^*\mathcal{D}c exp\left[-cc^* + c^*a + B_I(\phi_i, c)\right] = exp[B_i(\phi_i, a)] \tag{4.21}$$

and similarly for e_k. The two integrals over ξ and ξ' can be combined by redefining $\xi + \xi' \to \xi$. Doing the same for η and η' gives finally

$$\sigma_N(E) = \int \mathcal{D}\phi(x)\mathcal{D}\phi'(x)\mathcal{D}a_k^*\mathcal{D}a_k\mathcal{D}b_k^*\mathcal{D}b_k \mathrm{d}\eta\mathrm{d}\xi \mathrm{e}^W, \tag{4.22}$$

where

$$\begin{aligned} W = -iE\xi - iN\eta - \int \mathrm{d}^d k \Big(&\left[b_k^* b_k + a_k^* a_k \mathrm{e}^{-i\Delta_k}\right] + iS[\phi] - iS[\phi'] \\ &+ B_i(\phi_i, a) + B_f(\phi_f, b^*) + B_i(\phi_i', a)^* + B_f(\phi_f', b^*)^* \Big) \end{aligned} \tag{4.23}$$

and $\Delta_k \equiv \omega_k\xi + \eta$. Lastly the λ dependence must be separated if this is to be amenable to semiclassical techniques. Consider rescaling all quantities such that $\phi \to \sqrt{\lambda}\phi$ and $a_k \to \sqrt{\lambda}a_k$. The energy and particle number are rescaled as in 4.5. Dimensionally, from the kinetic term $S[\phi] \to S[\tilde{\phi}]/\lambda$ and therefore

$$W(E, N) = \frac{F(\epsilon, \nu)}{\lambda} \tag{4.24}$$

where $F(\epsilon, \nu)$ has no λ dependence. This implies

$$\sigma_N(E) = \int \mathcal{D}\phi(x)\mathcal{D}\phi'(x)\mathcal{D}a_k^*\mathcal{D}a_k\mathcal{D}b_k^*\mathcal{D}b_k \mathrm{d}\eta\mathrm{d}\xi \ \mathrm{e}^{F(\epsilon,\nu)} \tag{4.25}$$

which can by compared to the bounce from Chapter 3. In the previous case the lifetime was dominated by the minimum of the euclidean action. This was equivalent to finding the solution to the euclidean field equations. The current case is analogous; however ϕ can be complex and thus the simple Wick rotation will not be sufficient. If λ is small 4.25 will be dominated by the classical saddle-point solution (see Appendix B). This leaves the simple expression

$$\sigma_N(E) = exp\left[\frac{1}{\lambda}F(\epsilon, \nu)\right], \tag{4.26}$$

where now F has been redefined to correspond to the value of the exponent of the integrand at the saddle point. This expression will only give the exponential behaviour of the cross-section and should not be seen as giving any greater accuracy than this.

4.3 Boundary conditions

To proceed, the saddle point equations for each of the variables must be found. As discussed in Appendix B in this case these will be the values such that W is extremised. First consider the variation with respect to a_k

$$\begin{aligned}\frac{\delta W}{\delta a_k} &= 0 \\ &= -\int \mathrm{d}^d p \delta(\mathbf{k}-\mathbf{p}) \left[a_p^* \mathrm{e}^{-i\Delta_p} - a_{-p}\mathrm{e}^{-2i\omega_p T_i} + \sqrt{2\omega_p}\mathrm{e}^{-i\omega_p T_i}\phi_i(\mathbf{p})\right] \\ &= a_k^* \mathrm{e}^{-i\Delta_k} - a_k \mathrm{e}^{-2i\omega_k T_i} + \sqrt{2\omega_k}\mathrm{e}^{-i\omega_k T_i}\phi_i(\mathbf{k}).\end{aligned} \tag{4.27}$$

The saddle point of a_k^* may be found similarly to give the two equations

$$0 = a_k^* \mathrm{e}^{-i\Delta_k} - a_{-k}\mathrm{e}^{-2i\omega_k T_i} + \sqrt{2\omega_k} a_k \mathrm{e}^{-i\omega_k T_i}\phi_i(\mathbf{k}) \tag{4.28a}$$

$$0 = a_k \mathrm{e}^{-i\Delta_k} - a_{-k}^* \mathrm{e}^{2i\omega_k T_i} + \sqrt{2\omega_k} a_k \mathrm{e}^{i\omega_k T_i}\phi_i'(-\mathbf{k}) \tag{4.28b}$$

solving these simultaneous equations gives

$$a_k = \frac{\sqrt{2\omega_k}}{\mathrm{e}^{-i\Delta_k} - \mathrm{e}^{i\Delta_k}} \left[\phi_i'(-\mathbf{k}) - \mathrm{e}^{i\Delta_k}\phi_i(-\mathbf{k})\right] \mathrm{e}^{i\omega_k T_i} \tag{4.29a}$$

$$\overline{a}_k = \frac{\sqrt{2\omega_k}}{\mathrm{e}^{-i\Delta_k} - \mathrm{e}^{i\Delta_k}} \left[\phi_i(\mathbf{k}) - \mathrm{e}^{i\Delta_k}\phi_i'(\mathbf{k})\right] \mathrm{e}^{-i\omega_k T_i} \tag{4.29b}$$

As the solution is not necessarily real these saddle points are not required to be complex conjugates. Now the saddle point equations for ϕ_i are found. These are given by

$$0 = -i\dot{\phi}_i(\mathbf{k}) - \omega\phi_i(\mathbf{k}) + \sqrt{2\omega} a_{-k}\mathrm{e}^{-i\omega T_i} \tag{4.30a}$$

$$0 = i\dot{\phi}_i'(\mathbf{k}) - \omega\phi_i'(\mathbf{k}) + \sqrt{2\omega} a_k^* \mathrm{e}^{i\omega T_i} \tag{4.30b}$$

Using 4.29 and 4.30 the a_k and $\overline{a}_k$ terms may be solved leaving the initial boundary conditions

$$i\dot{\phi}_i(\mathbf{k}) + \omega\phi_i(\mathbf{k}) = \mathrm{e}^{i\Delta_k}\left[i\dot{\phi}_i'(\mathbf{k}) + \omega\phi_i'(\mathbf{k})\right] \tag{4.31a}$$

$$i\dot{\phi}_i(\mathbf{k}) - \omega\phi_i(\mathbf{k}) = \mathrm{e}^{-i\Delta_k}\left[i\dot{\phi}_i'(\mathbf{k}) - \omega\phi_i'(\mathbf{k})\right] \tag{4.31b}$$

Final state boundary conditions are also desired. Following the analogous procedure with the b-modes and ϕ_f andϕ_f' gives

$$0 = b_k^* - b_{-k}\mathrm{e}^{-2i\omega_k T_f} - \sqrt{2\omega_k} b_k \mathrm{e}^{-i\omega_k T_f}\phi_f'(\mathbf{k}) \tag{4.32a}$$

$$0 = b_k - b_{-k}^* \mathrm{e}^{2i\omega_k T_f} - \sqrt{2\omega_k} b_k \mathrm{e}^{-i\omega_k T_f}\phi_f(-\mathbf{k}) \tag{4.32b}$$

and

$$0 = i\dot{\phi}_f(\mathbf{k}) - \omega\phi_f(\mathbf{k}) + \sqrt{2\omega}b_k^* e^{i\omega T_f} \tag{4.33a}$$

$$0 = -i\dot{\phi}'_f(\mathbf{k}) - \omega\phi'_f(\mathbf{k}) + \sqrt{2\omega}b_{-k} e^{-i\omega T_f} \tag{4.33b}$$

However, these equations imply $\phi_f = \phi'_f$ and $\dot{\phi}'_f = \dot{\phi}_f$ and as their actions are identical they follow the same classical evolution between T_i and T_f. This means, in seeming contradiction to 4.31, that ϕ' and ϕ are in fact the same solution. The resolution of this apparent catastrophe is that the general saddle point solution is non-analytic and ϕ_i and ϕ'_i do not agree as they lie on different parts of the complex time plane. One may not be analytically continued to the sheet of the other due to the singularities between the sheets. The final saddle point solution required is for ξ and η which implicitly defines Δ_k via the equations

$$\epsilon = \int \mathrm{d}^d k \omega_k a_k^* a_k e^{-i\Delta_k} \tag{4.34a}$$

$$\nu = \int \mathrm{d}^d k a_k^* a_k e^{-i\Delta_k} \tag{4.34b}$$

which relate Δ_k to the energy and particle number.

4.4 Solving the BVP

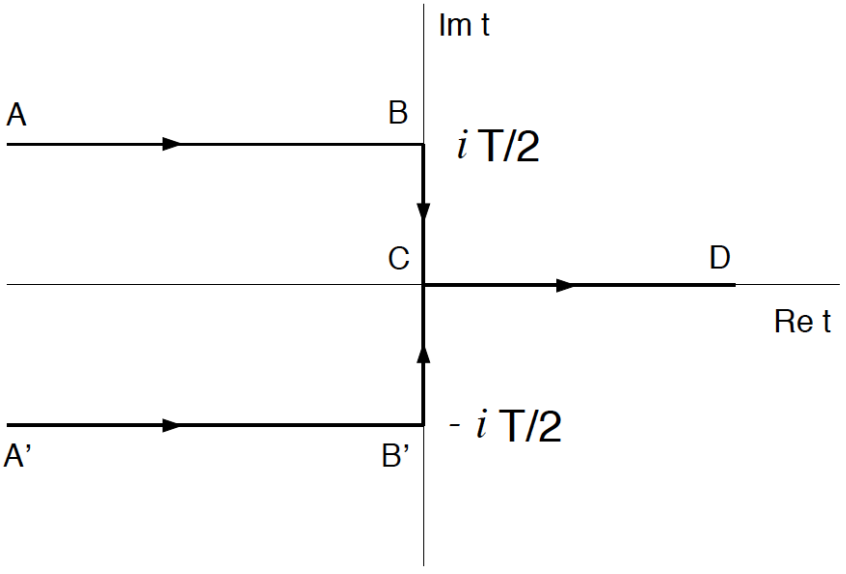

FIGURE 4.1: The contour taken in complex time. This will remove T from the boundary conditions

To progress, some simplifying results and assumptions must now be used. Firstly, consider ξ. By time translational symmetry the real part may be removed and so it may be considered a purely imaginary entity. For η the saddle point has been shown to be close to purely imaginary through lowest order perturbative calculations [25]. This means that the parameters may be written as

$$\xi = iT \tag{4.35a}$$

$$\eta = i\theta, \tag{4.35b}$$

implying that $i\Delta_k$ must be real. To remove T from the boundary conditions the integration contour may taken as shown in figure 4.1. This leaves $i\Delta_k \to -\theta$ in the initial boundary conditions. As $\tau \equiv Re(t) \to -\infty$, ϕ is defined on the line AB and ϕ' is defined on $A'B'$. While the fields are smooth near the contours it is expected that the space between these contours must contain singularities. Otherwise ϕ_i' could be continued to ϕ_i and the argument allowing for the apparent discrepancy for non-zero Δ_k would fail.

The second simplifying assumption is that the fields are linear in the limit of $\tau \to \pm\infty$. This implies the form for the fields

$$\phi(\mathbf{k}) = \frac{1}{\sqrt{2\omega_k}}\left[f_k \mathrm{e}^{-i\omega_k\tau} + g_k \mathrm{e}^{i\omega_k\tau}\right] \quad \text{on } AB \tag{4.36a}$$

$$\phi'(\mathbf{k}) = \frac{1}{\sqrt{2\omega_k}}\left[f_k' \mathrm{e}^{-i\omega_k\tau} + g_k' \mathrm{e}^{i\omega_k\tau}\right] \quad \text{on } A'B' \tag{4.36b}$$

as $\tau \to \infty$. Asymptotically the fields are analytic on their sheets and so in this limit

$$\phi'(\mathbf{k}) = \frac{1}{\sqrt{2\omega_k}}\left[f_k' \mathrm{e}^{-i\omega_k\tau+\omega_k T} + g_k' \mathrm{e}^{i\omega_k\tau-\omega_k T}\right] \quad \text{on } AB. \tag{4.37}$$

Substituting the form of the fields at initial time on AB into 4.31 gives

$$\begin{aligned} f_k' &= \mathrm{e}^{\theta} f_k \\ g_k' &= \mathrm{e}^{-\theta} g_k. \end{aligned} \tag{4.38}$$

Expressions for a_k and $\overline{a}_k$ must now be found using 4.29

$$\begin{aligned} a_k &= f_{-k} \\ \overline{a}_k &= g_k \mathrm{e}^{-\theta} \end{aligned} \tag{4.39}$$

and the expressions for energy and momentum can now be written

$$\begin{aligned} \epsilon &= \int \mathrm{d}^d k \omega_k f_{-k} g_k = \int \mathrm{d}^d k \omega_k f_k g_{-k} \\ \nu &= \int \mathrm{d}^d k f_{-k} g_k = \int \mathrm{d}^d k \omega_k f_k g_{-k} \end{aligned} \tag{4.40}$$

Taking the limit $\tau \to -\infty$ and neglecting contributions from rapidly oscillating terms (those proportional to $\exp(i \pm \omega_k \tau)$) the initial boundary terms may be simplified

$$B_i(\phi_i, a) = B_i^*(\phi_i', a) = \frac{1}{2} \int \mathrm{d}^d k f_{-k} g_k \tag{4.41}$$

The field at late times will also be linear and using 4.32 ϕ is written

$$\phi'(\mathbf{k}) = \phi(\mathbf{k}) = \frac{1}{\sqrt{2\omega_k}} \left[b_{-k} \mathrm{e}^{-i\omega_k \tau} + b_k^* \mathrm{e}^{-i\omega_k \tau} \right] \quad \text{on } CD \tag{4.42}$$

as $\tau \to \infty$. Using this the final boundary conditions are simply

$$B_i(\phi_i, a) = B_i^*(\phi_i', a) = \frac{1}{2} \int \mathrm{d}^3 k b_k^* b_{-k}. \tag{4.43}$$

The exponential factor will therefore become

$$F = \epsilon T + \nu\theta + iS[\phi] - iS'[\phi'] \tag{4.44}$$

where S and S' are evaluated on AB and $A'B'$ respectively. An additional step may be taken if the saddle-point solution is unique. In this case there is a symmetry analogous to CPT. The coefficients in the field equations are real and so $\Phi(\mathbf{x}, t) = \phi(\mathbf{x}, t^*)^*$ is also a solution. Uniqueness then implies $\phi(\mathbf{x}, t) = \phi(\mathbf{x}, t^*)^*$ but taking the partial Fourier transform this implies that $\phi = \phi'^*$ along the contours AB and $A'B'$. Therefore $f_k' = g_k^*$ and $g_k' = f_k^*$ and using 4.38 means

$$g_k = \mathrm{e}^{\theta} f_k^* \tag{4.45}$$

The energy and particle number saddle points are now therefore

$$\epsilon = \mathrm{e}^{\theta} \int d^3 k \omega_k f_k^* f_{-k} \tag{4.46a}$$

$$\nu = \mathrm{e}^{\theta} \int d^3 k f_k^* f_{-k} \tag{4.46b}$$

and the initial condition may be written as

$$\phi(\mathbf{k}) = \frac{1}{\sqrt{2\omega_k}} \left[f_k \mathrm{e}^{-i\omega_k \tau} + \mathrm{e}^{\theta} f_k^* \mathrm{e}^{i\omega_k \tau} \right] \quad on AB \tag{4.47a}$$

$$\phi'(\mathbf{k}) = \frac{1}{\sqrt{2\omega_k}} \left[\mathrm{e}^{\theta} f_k \mathrm{e}^{-i\omega_k \tau} + f_k^* \mathrm{e}^{i\omega_k \tau} \right] \quad on A'B' \tag{4.47b}$$

as $\tau \to \infty$. By the same symmetry the solution must be real along the CD line. This allows an additional boundary condition $Im(\phi(\mathbf{x}, t)) = Im(\dot{\phi}(\mathbf{x}, t)) = 0$. On the other hand the solution along the contours ABC and $A'B'C$ is generally complex (see later for a discussion of real solutions). The conjugation also implies that $S' = S^*$, giving the

final form of F

$$F(T,\theta) = \epsilon T + \nu\theta - 2ImS(T,\theta), \tag{4.48}$$

where there is no contribution from CD as the field is purely real here. As an additional check the saddle points satisfy

$$\frac{\partial F}{\partial T} = \frac{\partial F}{\partial \theta} = 0$$

which gives

$$\begin{aligned} \epsilon &= 2Im\frac{\partial \tilde{S}}{\partial T} \\ \nu &= 2Im\frac{\partial \tilde{S}}{\partial \theta}, \end{aligned} \tag{4.49}$$

where the $\tilde{S}$ indicates that this is taken at the saddle point of S. Equation 4.49 gives an additional consistency check for solutions. Therefore the problem has been reduced to finding solutions of the saddle points of the the action along the contour defined in figure 4.1 which satisfy the simple boundary conditions 4.47.

4.5 Forms of solution

4.5.1 Classical case

There are two distinct classes of solution to the saddle point equations: those that are classically allowed and those which require tunnelling. Consider first the classical case. This corresponds to propagation above the barrier at an energy $E > E_{sph}$ where E_{sph} is the energy of the wall. Note that this condition is necessary but not sufficient. A classical evolution implies that both the fields and the action will be real. Consider equation 4.31, if reality is required it is clear that Δ_k must be equal to zero. This implies that in this case $\phi_i(\mathbf{k}) = \phi'_i(\mathbf{k})$ and so the fields ϕ and ϕ' must lie on the same $(Im(t) = 0)$ line in the complex time plane for all time. Using this and taking $\Delta_k = 0$ in 4.29 gives

$$\begin{aligned} a_k &= \frac{\omega_k}{2}^{1/2}\phi_i(-\mathbf{k})\mathrm{e}^{i\omega_k T_i} \\ \overline{a}_k &= \frac{\omega_k}{2}^{1/2}\phi_i(\mathbf{k})\mathrm{e}^{-i\omega_k T_i} \end{aligned} \tag{4.50}$$

which are complex conjugates as required. Consider now 4.44: if fields are real and $T = 0$ then the action is also real and $S[\phi] = S'[\phi']$ and using $\Delta_k = 0$ for any k implies that T and θ are also zero. Therefore $F = 0$ and there is no exponential suppression. It is heartening to see this is the case as the suppression is due to tunnelling which could not occur in the classical case.

4.5.2 Periodic instantons

Consider the case $\theta = 0$. This corresponds to an unfixed initial particle number. The solution in this case is more physically intuitive. Equation 4.47 with $\theta = 0$ implies that the field is real in the infinite past along AB and A'B' and is thus real along the entirety of these contours. If the fields are also constrained to be real along BC and $B'C$ then this is the periodic instanton situation of [19]. Unlike the classical case this is not unsuppressed as $T > 0$. The form of the solution to this problem is much easier to understand than the general case and so it is discussed below.

First some remarks about the periodic instanton should be made. The periodic instanton is defined as a periodic solution to the Euclidean field equations. They can range from the sphaleron case (where the field remains near the false minimum) to the infinite period instanton discussed in Chapter 3. The smallest possible period for an instanton trajectory is decided by the form of the potential near the minimum (see [15] for the quantum mechanical case). Denote the periodic instanton solution $\Phi(\gamma, \mathbf{x})$ where γ is the euclidean time. The period (T) is decided by the starting energy and there must be two turning points such that $\dot{\Phi}(0, \mathbf{x}) = \dot{\Phi}(T/2, \mathbf{x}) = 0$. These conditions mean that it is possible to analytically continue the solution from the Euclidean region to the Minkowski region. This continuation will be the solution which satisfies the periodic instanton turning point conditions. The evolution will be Minkowski from $t = -\infty$ to the turning point, tunneling according to the euclidean field equations and then Minkowski evolution from another turning point to $t = \infty$. If the period is T then the time evolution follows the contour $ABCD$.

The $\theta = 0$ solution is real and so it is possible to deal with only ϕ along the upper contour $ABCD$. Consider what is meant by the saddle point solutions along this. The field is linear as $\tau \to \pm\infty$. This will then evolve according to the Minkowski field equations until the point $\tau = 0$. At this point the field propagates according to the Euclidean field equations for a time $T/2$. After this ϕ will return to evolving according to the Minkowski field equations. It can be easily seen that this is exactly the same set of equations as the periodic instanton and at least one of the saddle points must give this solution. It is shown in [19] that this solution is the saddle point which maximises $\sigma(E)$. If the initial and final fields may be written as

$$\phi_i(\mathbf{k}) = \frac{1}{\sqrt{2\omega}}(j_{-k}\mathrm{e}^{-i\omega_k\tau} + j_k^*\mathrm{e}^{i\omega_k\tau}) \tag{4.51a}$$

$$\phi_f(\mathbf{k}) = \frac{1}{\sqrt{2\omega}}(h_{-k}\mathrm{e}^{-i\omega_k\tau} + h_k^*\mathrm{e}^{i\omega_k\tau}), \tag{4.51b}$$

where the appropriate limits for τ are implied then the boundary conditions give

$$\begin{aligned} a_k &= j_k, \\ b_k^* &= h_k. \end{aligned} \tag{4.52}$$

Therefore the saddle points for the initial and final states are

$$\begin{aligned} |j\rangle &= exp\left[\int \mathrm{d}^3k f_k \hat{a}_k^\dagger\right]|0\rangle \\ \langle h| &= \langle 0|exp\left[\int \mathrm{d}^3k \hat{b}_k g_k^*\right] \end{aligned} \tag{4.53}$$

where j and h are determined by the periodic instanton. The saddle point for $\sigma(E)$ is equivalent to the probability of the transition between these states projected onto constant energy E. This is the energy of the periodic instantons.

Now consider the form of the cross-section at the saddle point. From 4.26 where $\theta = 0$

$$\sigma(E) = exp\left[-Im(S[\phi]) + ET\right] \tag{4.54}$$

but $Im(S[\phi])$ is just the Euclidean action of the periodic instanton. This is in fact the equivalent formula for false minimum decay in quantum mechanics at finite temperature. The transition probability is decided by the evolution in the Euclidean sector. As tunnelling decides the instability this sector can be seen as that in which the tunnelling occurs.

To conclude this section this analysis must be shown to be consistent with the derivation in Chapter 3. Consider the special case $a_k = b_k^* = 0$. From 4.50 this implies that $\phi_i = \phi_f = 0$ but then from 4.30 $\dot{\phi}_i = \dot{\phi}_f = 0$. The energy must be zero by 4.34a. Therefore this is a solution with a periodic instanton which starts and finishes at the same location with zero velocity and zero energy. This is clearly the infinite instanton bounce. Especially heartening is substituting $E = 0$ in 4.54 which implies the exponent for the transition probability has exactly the same suppression term as found using the Wick rotation.

In summary, in this special, $\theta = 0$, real solution case the field starts in the coherent state of the periodic instanton projected onto fixed energy E. It will then follow the path of the periodic instanton in the Euclidean sector and finally emerge at the coherent state of the end point of the periodic instanton. Note that energy must be fixed as increasing the energy will always increase the probability of transition. The general solution on the other hand may be complex on the contour ABC and A'B'C and the form of the field is much less simple. However properties such as conservation of energy before and after

the Euclidean evolution allow a handle to be kept on this case. In the next section the development of this formalism such that solutions may be found numerically is explored.

Chapter 5

Translation to a numerical problem

Many features of false vacuum decay can be seen in analytically (partially) solvable cases: see for example [24], [26], [27]. For this project, however, the problem is treated numerically. The false vacuum decay is translated to the lattice using the methods employed in [28] and [29]. Similar studies have been carried out in [30] and [9] which motivated the work for this project. Numerical studies can be used to find properties of the suppression exponent. A $(1+1)$ dimensional case is explicitly considered and transferred to a two dimensional lattice. This makes the problem numerically tractable. Each point (i, j) on the lattice corresponds to a particular (t_i, x_j). The field ϕ has a value at each point $\phi(i, j)$ which corresponds to its value at a particular time and position. Both the cases of spontaneous false vacuum decay and induced vacuum decay will be translated to this lattice formulation. As the solution in d dimensions will be dependent on only r and t most of these results can be trivially extended for a d dimensional analysis. Therefore unless $d = 1$ must be explicitly taken, it is left arbitrary.

5.1 Properties of the lattice

Consider a lattice which covers a space $L_x \times L_t$ and has $n_x + 1$ spacial sites and $n_t + 1$ time sites. Periodic boundary conditions are applied for the spacial direction such that the site $j = N + 1$ is defined as $j = 0$ and $j = -1$ defined as $j = N$. The spacings in

the t direction are given by

$$\begin{aligned} \mathrm{d}t_i &= t_{i+1} - xii = 0, ..., n_{t-1} \\ \mathrm{d}\tilde{t}_i &= (\mathrm{d}t_{i-1} + \mathrm{d}t_i)/2 i = 1, ..., n_{t-1} \\ \mathrm{d}\tilde{t}_{n_t/0} &= \frac{\mathrm{d}t_{n_t - 1/0}}{2} \end{aligned}$$

where the tilde indicates that the spacing is to be associated with links while untilded is associated with sites [29]. $\mathrm{d}x_j$ and $\mathrm{d}\tilde{x}_j$ are defined similarly but due to the periodic boundary conditions n_x and 0 are no longer special cases. The positions $x_j \in [0, ..., L_t]$ and $|t_i| \in [0, ..., L_x]$. Depending on the problem, t_i will be complex in different regions. For the bounce, for example, it is purely imaginary. The action is rescaled to seperate the coupling constant and the result may be discretised as

$$S[\phi] = \sum_{ij} \left[\frac{1}{2}(\phi_{i+1,j} - \phi_{i,j})^2 \frac{\mathrm{d}\tilde{r}_j}{\mathrm{d}t_i} - \frac{1}{2}(\phi_{i,j+1} - \phi_{i,j})^2 \frac{\mathrm{d}\tilde{t}_i}{\mathrm{d}x_j} - V_{ij} \mathrm{d}\tilde{t}_i \mathrm{d}\tilde{x}_j \right] \tag{5.1}$$

where all the terms have been rescaled implicitly. Depending on the problem there will also be boundary conditions implemented at the initial and final times which will be made explicit later. The equation to be solved in intermediate times is $\delta S/\delta\phi = 0$ with lattice equivalent

$$\frac{\partial S}{\partial \phi_{ij}} = 0. \tag{5.2}$$

While the bounce scenario can be reduced to a one dimensional equation the solution to the particle production problem is a boundary value problem that must be solved over the entire lattice. These equations are everywhere non-linear. The bounce thus forms a useful check for more complicated situations. The approach used to solve this lattice of non-linear equations is a multidimensional analogue of the Newton-Raphson method. As will be shown this allows the problem to be transformed into a set of linearised equations which adjust ϕ at every iteration to approach the solution. The main drawback of this method is that the existence of zero-modes may spoil the convergence [28].

Consider a general function $f(\phi_{ij})$. The solution sought is the one such that $f(\phi_{ij}) = 0$. Using a Taylor expansion gives

$$f(\phi_{ij} + h_{ij}) = \frac{\partial f(\phi_{ij})}{\partial \phi_{kl}} u_{kl} + f(h_{ij}) \tag{5.3}$$

where h_{ij} is a small shift, $u_{ij} = \phi_{ij} - h_{ij}$ and normal summation convention used. Now consider setting $f(\phi_{ij} + h_{ij}) = 0$. Rearranging this expression gives

$$\frac{\partial f(\phi_{ij})}{\partial \phi_{kl}} u_{kl} = -f(h_{ij}) \tag{5.4}$$

which can be written as $L.u = d$. In the Newton-Raphson technique u_{ij} corresponds to the correction of the field which should bring ϕ_{ij} closer to solving $f(\phi_{ij}) = 0$. This will now be applied to the case of the scalar field. In this situation L has dimension $(n_t + 1)(n_x + 1) \times (n_t + 1)(n_x + 1)$ while u and d have dimension $(nt + 1)(nx + 1)$. The equations considered are $f(\phi_{ij}) = \partial S/\partial\phi_{ij}$ at intermediate times and boundary terms which depend on the explicit problem. To turn these equations into an algorithm that can be implemented numerically it is useful to make the j index implicit and consider a system of $(n_t + 1)$ vectors of dimension $(n_x + 1)$ denoted $\mathbf{u}_i$ and $\mathbf{d}_i$. For the case of the scalar field the equations being solved will contain no higher than second order derivatives in ϕ and this means L may be split into three blocks: the diagonal $(D_i)_{jk}$ and the off-diagonals $D_i^{(+)}$ and $D_i^{(-)}$. These each have dimension $(n_x + 1)(n_x + 1)$ and are defined by

$$\begin{aligned}(D_i)_{jk} &= \frac{\partial f(\phi_{ij})}{\partial \phi_i k} \\ (D_i^{(+)})_{jk} &= \frac{\partial f(\phi_{ij})}{\partial \phi_{i+1,k}} \\ (D_i^{(-)})_{jk} &= \frac{\partial f(\phi_{ij})}{\partial \phi_{i-1,k}}\end{aligned} \tag{5.5}$$

Clearly $D_i^{(-)}$ and $D_i^{(+)}$ are zero at $i = 0, nt$ respectively. Using these 5.4 may be rewritten as the set of equations

$$\begin{aligned} D_0\mathbf{u}_0 + D_0^{(+)}\mathbf{u}_1 &= \mathbf{d}_0 \\ &\dots \\ D_i^{(-)}\mathbf{u}_{i-1} + D_i\mathbf{u}_i + D_i^{(+)}\mathbf{u}_{i+1} &= \mathbf{d}_i \\ &\dots \\ D_n t^{(-)}\mathbf{u}_{nt-1} + D_n t\mathbf{u}_n t &= \mathbf{d}_{nt}\end{aligned} \tag{5.6}$$

where the first and last of these equations contain the boundary conditions. A set of matrices and vectors A_i and $\mathbf{b}_i$, $i = 0, .., nt - 1$ are defined by

$$\mathbf{u}_i = A_i\mathbf{u}_{i+1} + \mathbf{b}_i, \tag{5.7}$$

where the dimensions of A_i and b_i are clear from the formula. The first equation in 5.6 implies

$$A_0 = -[D_0]^{-1}D_0^{(+)}\mathbf{b}_0 = [D_0]^{-1}d_0. \tag{5.8}$$

Now for the intermediate times 5.6 and 5.7 allow recursive expressions for A_i and $\mathbf{b}_i$ to be found

$$A_i = -[D_i^{(-)} A_{i-1} + D_i]^{-1} D_i^{(+)} \tag{5.9}$$
$$b_i = [D_i^{(-)} A_{i-1} + D_i]^{-1} [\mathbf{d}_i - D_i^{(-)} b_{i-1}]. \tag{5.10}$$

An explicit equation for $\mathbf{u}_{n_t}$ may then found.

$$\mathbf{u}_{n_t} = [D_{n_t}^{(-)} A_{n_t-1} + D_{n_t}]^{-1} [\mathbf{d}_{n_t} - D_{n_t}^{(-)} \mathbf{b}_{n_t-1}] \tag{5.11}$$

Knowing this along with 5.7 allows all of $\mathbf{u}_i$ to be calculated. The field is then corrected in the k_{th} iteration as

$$\phi_{ij}^{(k+1)} = \phi_{ij}^{(k)} + u_{ij} \tag{5.12}$$

and the process is repeated with this new value for the field at all points.

5.2 Boundary conditions

The bounce has trivial boundary conditions but the induced vacuum decay requires more work. In Chapter 4 the boundary conditions for ϕ were found to be (for an appropriate contour in imaginary time)

$$Im(\dot{\phi}(0, \mathbf{x})) = Im(\phi(0, \mathbf{x})) = 0 \tag{5.13}$$
$$g_k = \mathrm{e}^{-\theta} f_{-k}^* \tag{5.14}$$

and the action is extremised at intermediate times. The initial field is

$$\phi(\mathbf{k}) = \frac{1}{\sqrt{2\omega_k}} \left[f_k \mathrm{e}^{-i\omega_k \tau} + \mathrm{e}^{\theta} f_k^* \mathrm{e}^{i\omega_k \tau} \right] \tag{5.15}$$

Defining $\gamma \equiv \mathrm{e}^{-\theta}$ this may be expanded to give

$$\begin{aligned} (\sqrt{2\omega_k}) Re(\phi(\mathbf{k})) \frac{\gamma}{1+\gamma} &= Re(f_k) \cos(\omega_k \tau) + Im(f_k) \sin(\omega_k \tau) \\ (\sqrt{2\omega_k}) Im(\phi(\mathbf{k})) \frac{\gamma}{1-\gamma} &= Im(f_k) \cos(\omega_k \tau) - Re(f_k) \sin(\omega_k \tau) \end{aligned} \tag{5.16}$$

Using this, the energy and particle number saddle points may be rewritten in terms of $\phi(k)$ [29]

$$E = \int \mathrm{d}^d k \omega_k^2 \left(\frac{2\gamma}{(1+\gamma)^2} Re(\phi(\mathbf{k}))Re(\phi(-\mathbf{k})) + \frac{2\gamma}{(1+-\gamma)^2} Im(\phi(\mathbf{k}))Im(\phi(-\mathbf{k})) \right) \tag{5.17a}$$

$$N = \int \mathrm{d}^d k \omega_k \left(\frac{2\gamma}{(1+\gamma)^2} Re(\phi(\mathbf{k}))Re(\phi(-\mathbf{k})) + \frac{2\gamma}{(\gamma-1)^2} Im(\phi(\mathbf{k}))Im(\phi(-\mathbf{k})) \right) \tag{5.17b}$$

As an infinite BC cannot be implemented numerically, unlike previously the limit $\tau \to -\infty$ cannot be taken and the boundary terms which involve τ must be considered. The additional term in F turns out to be [28]

$$- Re(\frac{1}{2} \int \mathrm{d}^3 k (f_k f_{-k} \mathrm{e}^{-2i\omega_k \tau} - f_k f_{-k} \mathrm{e}^{2i\omega_k \tau}). \tag{5.18}$$

Changing variables again to $\phi(k)$ changes the suppression to [29]

$$\begin{aligned} F(\epsilon, \nu) = N\theta + ET - 2Im(S[\phi]) - \frac{1-\gamma}{1+\gamma} \int \mathrm{d}^d k \omega_k Re(\phi_i(\mathbf{k}))Re(\phi_i(-\mathbf{k})) \\ + \frac{1+\gamma}{1-\gamma} \int \mathrm{d}^d k \omega_k Im(\phi_i(\mathbf{k}))Im(\phi_i(-\mathbf{k})) \end{aligned} \tag{5.19}$$

where there is now an additional boundary term in comparison to 4.54.

5.3 Translation to the lattice

The final step before the algorithm may be implemented is turning the boundary terms into lattice equations. This is standard for the end conditions but for 5.19 requires more work. Assuming the false minimum lies at $\phi = 0$ and rescaling the terms such that $V''(0) = 1$, the quadratic part of the action may be written (leaving time continuous)

$$S_{quad} = \int \mathrm{d}t \sum_j \left(\frac{1}{2} \dot{\phi}_j^2 \mathrm{d}\tilde{x}_j - \frac{(\phi_{j+1} - \phi j)^2}{2\mathrm{d}_j} - \frac{1}{2} \phi_j^2 \mathrm{d}\tilde{x}_j \right) \tag{5.20}$$

where $\phi_j = \phi(t, x_j)$. Consider the canonical form of the action

$$S = \int \mathrm{d}t \sum_j \left(\dot{\chi}_j^2 + h_{jk} \chi_j \chi_k \right) \tag{5.21}$$

Defining $\chi_j(t) = \phi_j(t)\sqrt{\mathrm{d}x}$ it can be seen that 5.20 is in this form if the Hamiltonian operator is given by

$$h_{jk} = \delta_{jk}\left(\frac{1}{\mathrm{d}\tilde{x}_j \mathrm{d}x_{j-1}} + \frac{1}{\mathrm{d}\tilde{x}_j \mathrm{d}x_j} + 1\right) - \frac{\delta_{j+1,k}}{\mathrm{d}x_j\sqrt{\mathrm{d}\tilde{x}_j \mathrm{d}\tilde{x}_k}} - \frac{\delta_{j-1,k}}{\mathrm{d}x_j\sqrt{\mathrm{d}\tilde{x}_j \mathrm{d}\tilde{x}_k}} \tag{5.22}$$

By diagonalising h_{jk} the eigenfunctions ζ_k^n and eigenvalues ω_n which replace the plane waves and frequencies ($\omega_k = \sqrt{k^2+1}$) occurring in 5.19 may be found. Therefore the partial Fourier transform becomes

$$\phi(\mathbf{k}) = \int \frac{\mathrm{d}^3k}{(2\pi)^{3/2}} \mathrm{e}^{-i\mathbf{k}.x}\phi\mathbf{k} \rightarrow \sum_j \zeta_j^n \chi_j = \sum_j \zeta_j^n \sqrt{\mathrm{d}\tilde{x}}\phi_{ij}. \tag{5.23}$$

As integrals over $\mathbf{k}$ now correspond to sums over n the boundary term my be rewritten as

$$\sum_{jk} \Omega_{jk}\left(-\frac{1-\gamma}{1+\gamma}Re(\phi_{0j})Re(\phi_{0k}) + \frac{1+\gamma}{1-\gamma}Im(\phi_{0j})Im(\phi_{0k})\right) \tag{5.24}$$

where

$$\Omega_{jk} = \sum_n \sqrt{\mathrm{d}\tilde{x}_j}\zeta_j^n \omega_n \zeta_k^n \sqrt{\mathrm{d}\tilde{x}_j} \tag{5.25}$$

and therefore the form of the equation that must be solved at initial times is

$$\frac{\partial S}{\partial \phi_{0j}} + \sum_k \Omega_{jk}\left(i\frac{1-\gamma}{1+\gamma}Re(\phi_{0k}) - \frac{1+\gamma}{1-\gamma}Im(\phi_{0k})\right) = 0. \tag{5.26}$$

The final boundary conditions ($Im(\phi(0,\mathbf{x})) = Im(\dot{\phi}(0,\mathbf{x})) = 0$) are simply [28]

$$Im(\phi_n t, j) = Im(\frac{\partial S}{\partial \phi_{nt,j}}) = 0 \tag{5.27}$$

The case for a general lattice with non-equal spacings has been discussed. It should be mentioned however that in the case of constant spacial spacing the eigenfunctions simplify to

$$\zeta_k^n = \mathrm{e}^{-i(\omega_n r_k + \rho)} \tag{5.28}$$

where ρ is just a phase. This is equivalent to the continuous form. The eigenvalues are given by

$$\omega_n = \frac{2}{\mathrm{d}x}\sin\left(\frac{n\mathrm{d}x}{2}\right) \tag{5.29}$$

where $\mathrm{d}x$ is the lattice spacing.

The theoretical problem has now been set up and transformed to an algorithm that can be implemented on the lattice. In the next section the results of this will be used to begin finding numerical solutions to the decay of the false vacuum. This is a critical starting point to solving the more complex induced vacuum decay. The final point to

be noted is that for the case of kink-anti-kink production with degenerate minima there is no potential barrier separating the SA pair from the particle sector [9] and so this case cannot be treated as potential tunnelling. However by slightly deforming one of the minima by $\delta\rho$ to create a false vacuum the problem becomes that of a tunnelling process. The limit $\delta\rho \rightarrow$ is taken at the end of the calculation. This is done by continuing the solution for small $\delta\rho$ found numerically. The expected end result is shown in [9] to be two widely separated kinks with total energy $E_{cb} = 2M_s$. Where M_s is the mass of the kink.

Chapter 6

First Numerical Results

The use of lattice simulations for false vacuum decay is relatively new and there are hazards such as the existence of zero modes which spoils convergence and the negative mode which can destabilise the entire process. Because of this it is wise to start with the simplest case of QM and then move on to the field theory case for spontaneous decay. This lays the groundwork for which can be built on for the higher complexity induced decay problem to build on.

6.1 Quantum mechanics

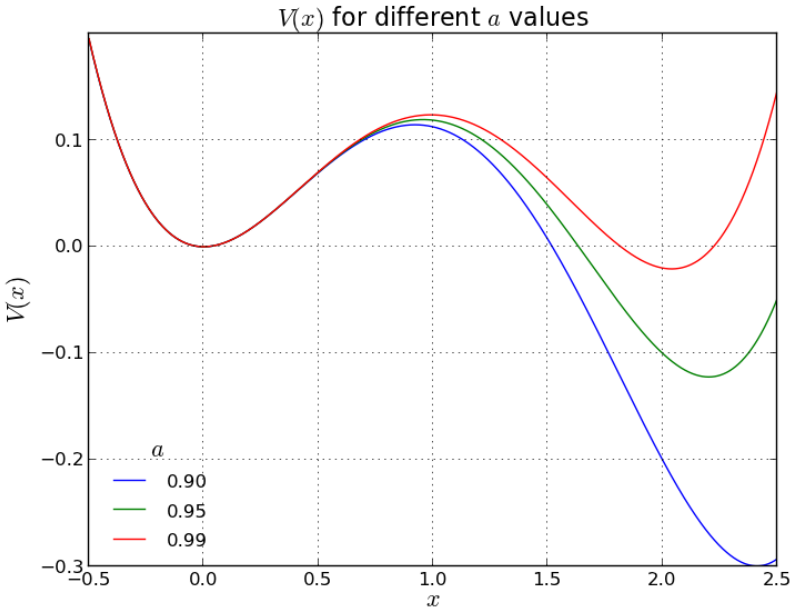

FIGURE 6.1: The potential used for various values of a.

As a starting point the analytically solvable quantum mechanic case is considered. The potential chosen is

$$V(x) = \frac{1}{2}x^2 - \frac{1}{2}x^3 + \frac{a}{8}x^4 \tag{6.1}$$

Which is shown for some values of a in figure 6.1. This potential has a false minimum at $x = 0$ and the bounce will occur at

$$x_0 = \frac{2 - 2\sqrt{1-a}}{a}. \tag{6.2}$$

The solution must be symmetric and thus only half of the bounce need be found. The boundary conditions

$$\begin{aligned} x(L_t) &= 0 \\ \dot{x}(0) &= 0 \end{aligned} \tag{6.3}$$

are applied. The first case considered is $a = 0.99$ and the initial guess is found by the solving 2.9 using Mathematica. This also allows the time length (L_t) to be set as it must be larger than the time for the bounce to occur and was taken to be $L_t = 10$ and $n_t = 500$. The Newton-Raphson iteration was run 15 times where the maximum deviation from $\delta S/\delta\phi = 0$ was found to be of order $\mathcal{O}10^{-13}$. The value of a was changed to $a = 0.98$ and the solution to $a = 0.99$ was then used as the initial guess. This was repeated as a was lowered to find the solution for a range of values in a. Some sample solutions are shown in figure 6.2 The purpose of this analysis is to find the behaviour of

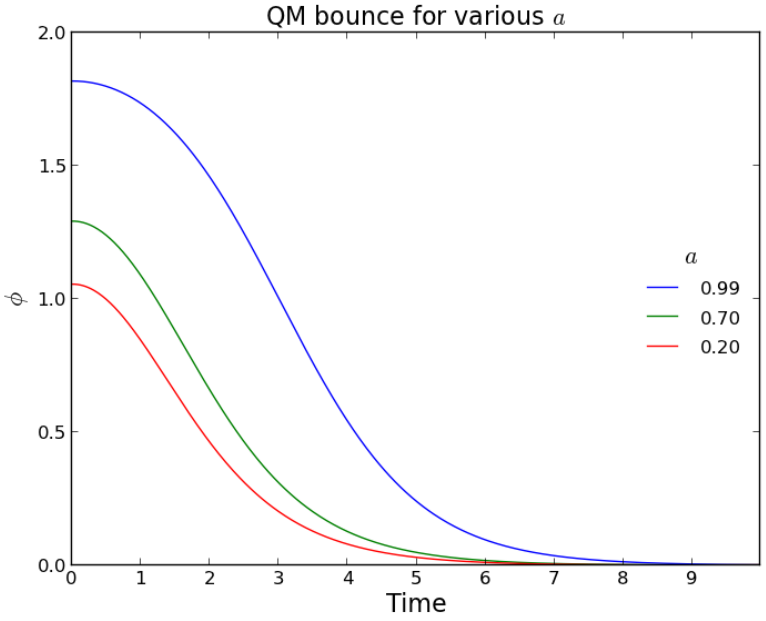

FIGURE 6.2: The solutions found for different values of a. The main feature is that the time taken is greater for higher a.

the suppression exponent in the decay time. As shown in Chapter 2 this is given by S_0.

By using 5.1 this is calculated for each of the solutions (remembering that the result must be doubled as the solution found is only half of the bounce). A plot of the suppression against a is then made and shown in 6.3(a). This shows a monotonical increase as $a \to 1$. The reason for the form of the dependence can be found by considering the height of the barrier. As shown in 6.3(b) this height increases with a and plotting the suppression against barrier height shows that as expected transitions will become less and less likely as this height is increased. This is physically as expected – the higher the barrier the less likely the tunnelling. The near linear relation between action and height is also encouraging as the tunnelling rate should be exponentially suppressed by the height. This can be validated against another way of finding the bounce action,

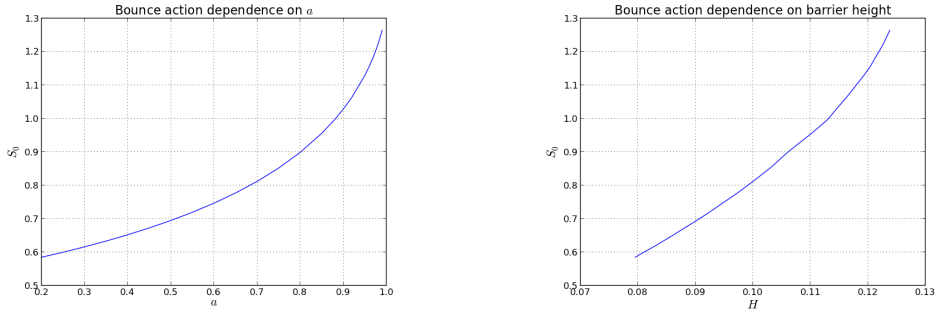

(a) Suppresion against a

(b) Suppression against height

FIGURE 6.3: LEFT:The suppression in the exponent is given by S_0. As shown this increases with a reducing the probability of a transition to occur. RIGHT: The suppression is shown to increase with the barrier height as expected.

2.36. Using Mathematica this was calculated and compared to the result found from the explicit numerical form of the bounce. This was found to be in agreement with an average fractional error of 7×10^{-6}. This validates the approach and now the more complicated case of a $(1+1)$ dimensional field may be considered. After the bounce the particle moves classically with the initial conditions $x(0) = x_0$ and $\dot{x}(0) = 0$. This behaviour is shown in figure 6.4 for $a = 0.70$.

6.2 Bounce in scalar field theory

To further ensure the validity of the code a problem of higher complexity was then attempted. The bounce solution can be solved as a 1D equation (see 3.16) but by attempting to solve it on the lattice insight may be gained into the prospects of extending to the case of induced vacuum decay. This is a relatively new area and so it is important to see how attempts at solving the problem on the lattice fare. Various probes discussed in Chapter 4 will allow a handle to be kept on the solutions. The potential considered

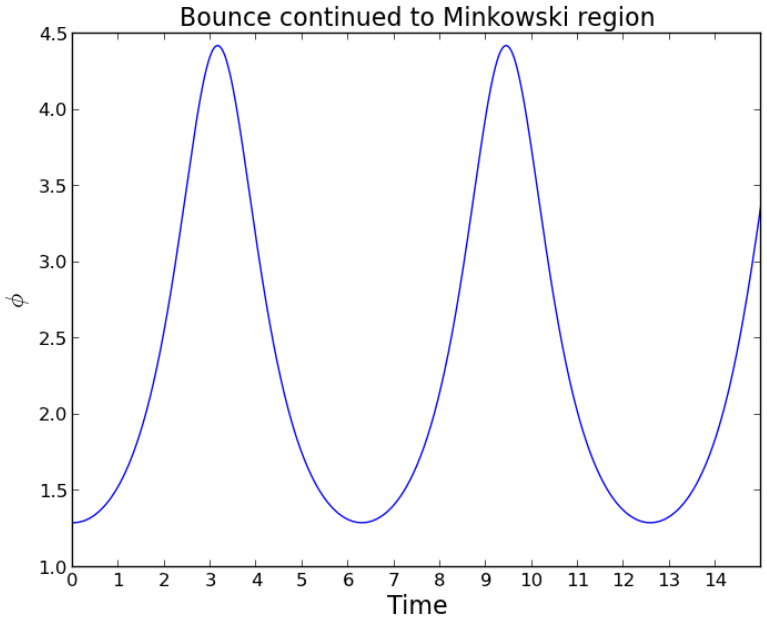

FIGURE 6.4: The Minkowski solution found for $a = 0.7$. The particle propagates away from the tunnelling exit with E=0.

is the field analogue of 6.1

$$V(\phi) = \frac{1}{2}\phi^2 - \frac{1}{2}\phi^3 + \frac{a}{8}\phi^4 \tag{6.4}$$

The following boundary conditions are applied

$$\begin{aligned} \phi(0, j) &= \phi(1, j) \\ \phi(n_t, j) &= 0. \end{aligned} \tag{6.5}$$

These are sufficient to converge on the bounce solution providing the initial guess is appropriately chosen. The lattice used had the parameters: $n_x = 50$,$n_t = 250$, $L_t = L_x = 40$. These were set such that the critical region of each solution would comfortably fit. The potential was then considered with $a = 0.97, 0.95, 0.9, 0.7, 0.5$. The existence of zero modes (which are nearly zero on the lattice) means that there is a continuous set of approximate solutions [29]. Therefore, the initial guess must be close so that the algorithm will converge. To ensure this Mathematica was used to find the appropriate solution to 3.16 using the overshoot-undershoot method. This was then applied as the initial guess. The solution typically converged in about 4-5 steps to maximum deviation from $\delta S/\delta\phi = 0$ of order $\mathcal{O}10^{-7}$. The solutions for the extremal values considered, $a = 0.97$ and $a = 0.5$, are shown in figure 6.5(a) and 6.5(b) respectively. These plots show that the solution is, as expected, radial. The boundary conditions are insufficient to remove translational invariance. To illustrate this two different solutions were found

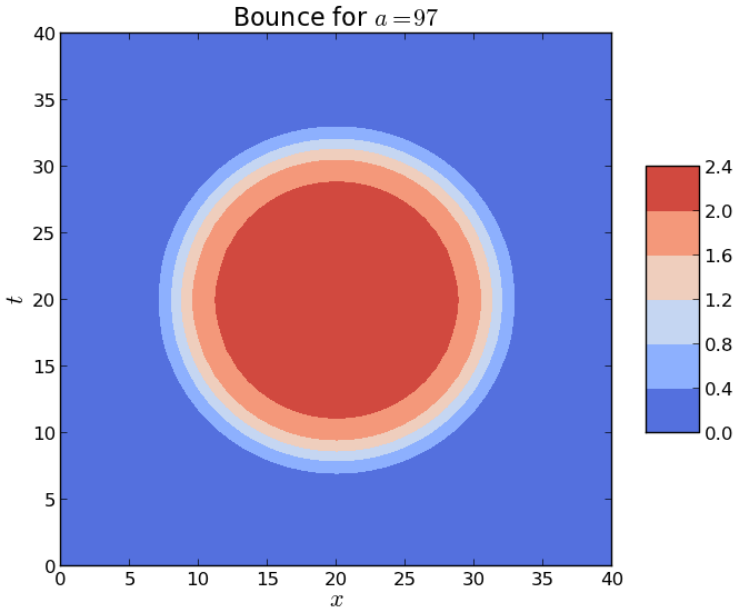

(a) Instanton solution for a =0.97

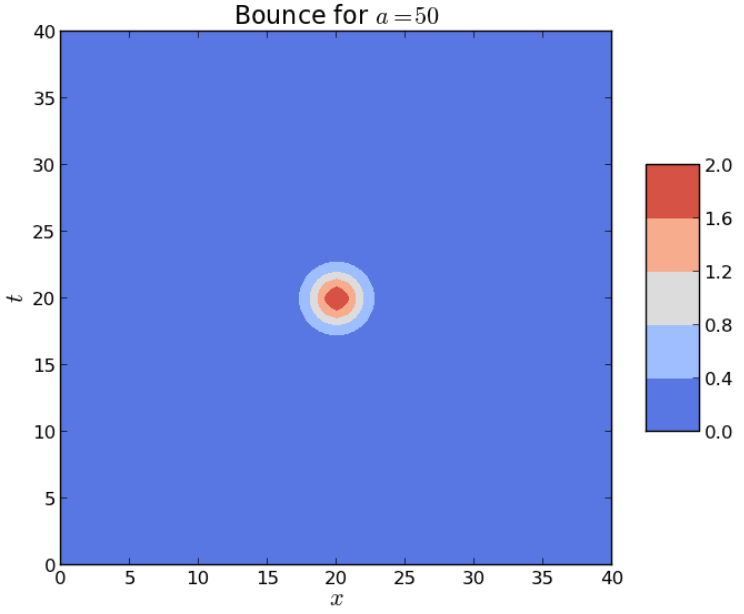

(b) Instanton solution for a =0.50

FIGURE 6.5: Contour plots for extremal a values. It is clear that the larger a solution must stay near the end point for longer and this means the critical bubble is larger. Note different colour scales.

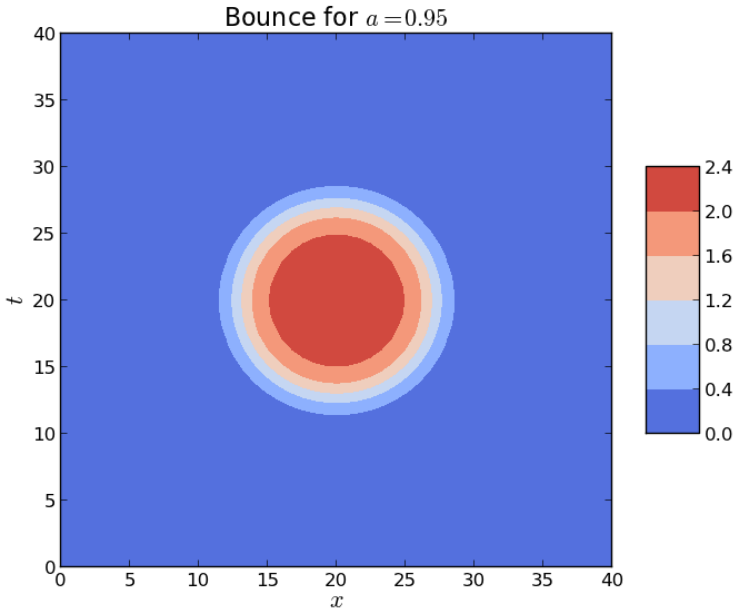

(a) Instanton solution in centre

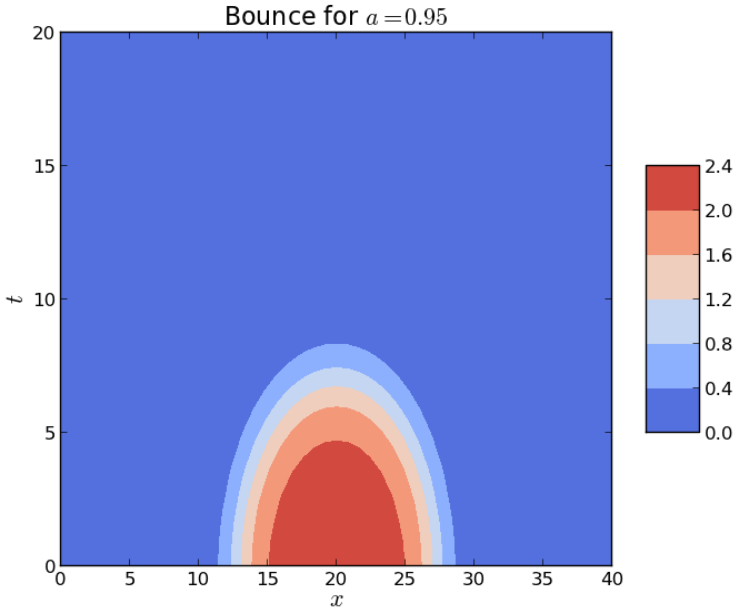

(b) Instanton solution at start

FIGURE 6.6: Contour plots with bounce in different positions. This shows the translational invariance.

for $a = 0.95$. These are shown in figure 6.6(a) and 6.6(b). All of these plots exhibit only radial behaviour for ϕ. This means that the path may be represented by one line. Using this fact, the different bounce solutions can be represented as functions of $r = \sqrt{x^2 + t^2}$. This is done in figure 6.7. As $a \to 1$ the potential becomes flatter and for $a = 1$ is a symmetric double well. This means that in this limit the thin wall approximation is

valid. Figure 6.7 shows that the field remains near the true vacuum position for higher values of a. This is as expected as for $a = 1$ the time spent at the other vacuum must be infinite. To check the solution and validate the method the Hamiltonian

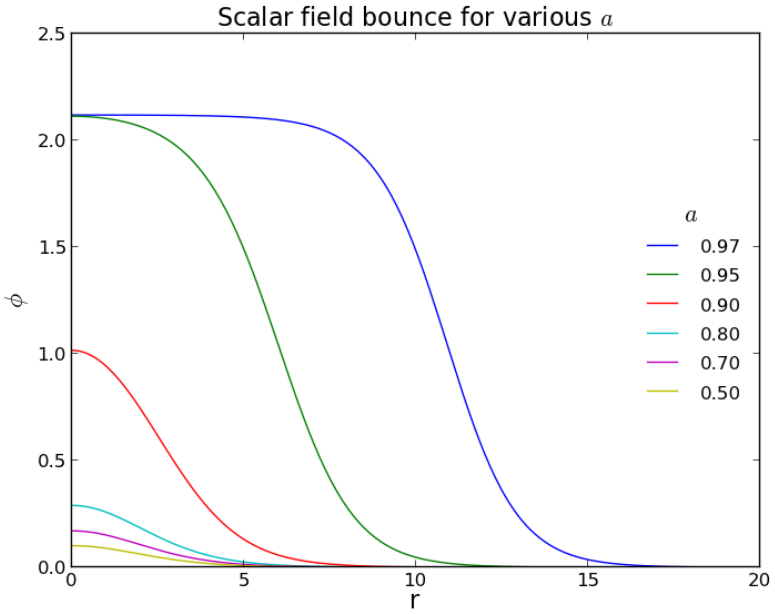

FIGURE 6.7: The scalar field bounce for various values of a. As a approaches 1 the thin wall approximation becomes valid.

$$H = \int \mathrm{d}x \frac{1}{2}\frac{\partial\phi}{\partial\tau}^2 - \frac{1}{2}\nabla\phi^2 - V(\phi) \tag{6.6}$$

was calculated and found to be consistently within a small margin of 0. This is required for the instanton as this is a zero energy solution. The Hamiltonian for $a = 0.95$ is shown in figure 6.8. The scale is small compared to the kinetic and potential energies ($\mathcal{O}(10^1)$). The small variations correspond to points with large derivatives. To keep the simulation from taking an unreasonable time the lattice used has quite large x spacings and so these small deviations are to be expected. A last measure can be found using the energy in equation 5.17a. This was seen to be zero as expected for the instanton solution. With the confidence that the solution behaves as expected, the action for the bounce may now be found and thus the expression exponent estimated. As the action at the false vacuum is null this may be done from only considering the region of the critical bubble. The resulting distribution is shown in figure 6.9. This shows that the suppression, as compared to the 1D QM case, is again increasing with time. However, the action is now both much higher than before and increases much faster with a. This means that the decay is far less likely to occur than for one dimensional quantum mechanics. This is to be expected however due to the 'drag' term in 3.16. It is also to be expected physically as it is more energetically viable to create a bubble in lower dimensions. This can be

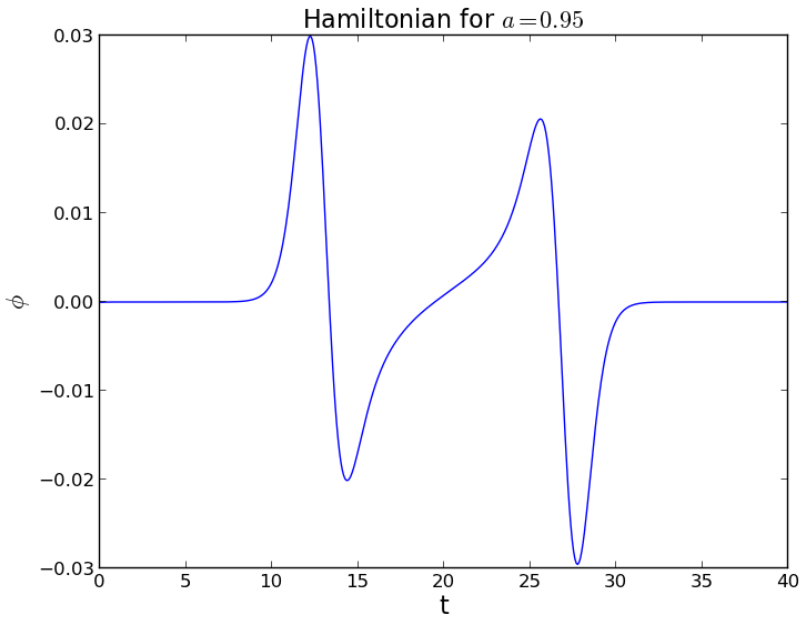

FIGURE 6.8: The behaviour shows deviation from 0 within expected bounds from accuracy of lattice

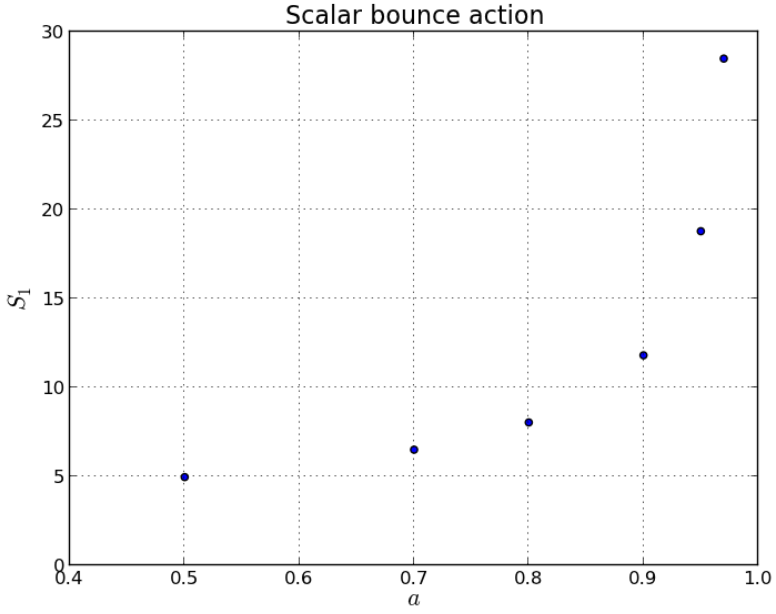

FIGURE 6.9: The suppression increases as $a \to 1$. This is because the height of the barrier is increased.

compared to domain wall propagation in, for example, the Ising model [31]. The effect of higher dimensions is that more of the field must be forced into the bubble configuration and thus it is less likely to occur. These results were compared to those calculated from Mathematica and the action was found to agree on the order $\mathcal{O}(10^{-}3)$.

Finally the results are compared to the thin wall approximation. S_1 was calculated in this approximation for $d = 3$ in Chapter 4. The case of $d = 1$ is analogous with the result

$$\begin{aligned} R &= \frac{S_0}{\epsilon} \\ S_1 &= \frac{\pi S_0^2}{\epsilon} \end{aligned} \tag{6.7}$$

where S_0 is the QM bounce action and ϵ is the height difference between the barriers. In this potential $V''(0) \simeq 1$ and the condition for the thin wall approximation to be valid is therefore $R >> 1$. It is therefore clear that this limit cannot apply to $a < 0.9$. For the case of higher a it is interesting to see if this approximation can be stretched to give results in agreement with 6.9. The values of R estimated for these paths from 6.7 for $a = 0.90, 0.95$ and 0.97 are $1.7, 4.6, 8.9$ respectively, which by looking at 6.7 is qualitatively quite accurate. The critical action evaluated for these points from6.7 is $S_1 = 2.8, 8.22, 16.25$ which compared to 6.9 is a large underestimate for $a = 0.97$ and worse for the others. This can be understood by revisiting the approximation. As the wall was taken to be thin the positive part of the integral only looked at $r = R$. However, from the plot it can be seen that this is not valid and as R also underestimates the result will be too small. Therefore the thin wall scenario is not appropriate to describe these cases. It should be noted, however, that the rapid fall off of the action with decreasing a is also seen in this approximation suggesting general features can still be found in this region.

Finally, the solution was attempted to be continued into the Minkowski region. This had very limited results mainly due to the effects of the negative mode and the size of the lattice. The result for $L_t = 3$ continuation of $a = 0.95$ is shown in figure 6.10. The initial guess is just the extension of the bounce for the entire time. As can be seen the radius stays approximately constant. This is because the time for which it was possible to continue the solution without experiencing divergences is very short (much shorter than the radius of the bounce). These divergences can be seen in the attempted continuation of $a = 0.90$ for $L_t = 2$ in figure 6.11. There was not time to correct this problem which may be due to the negative mode or simply the numerical accuracy of the matrix package. While this evolution is important, it should be noted that the decay has no dependence on it.

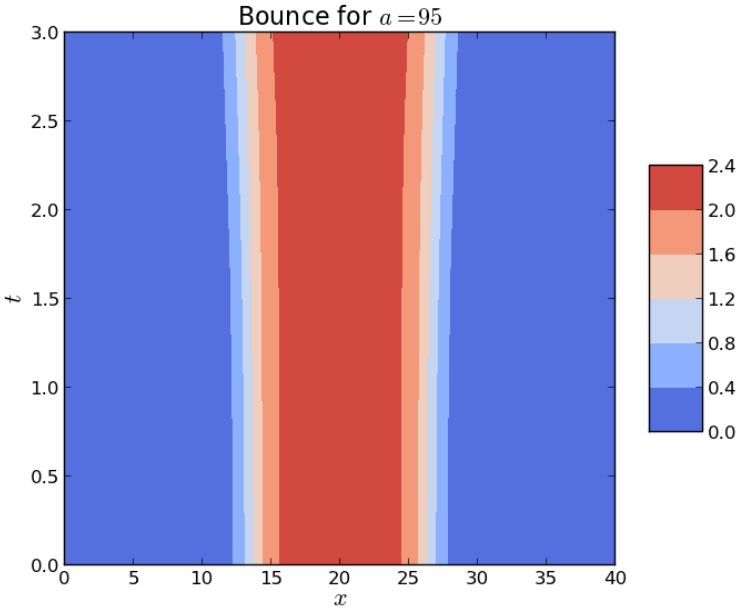

FIGURE 6.10: The Minkowski extension of the bounce for a=0.95

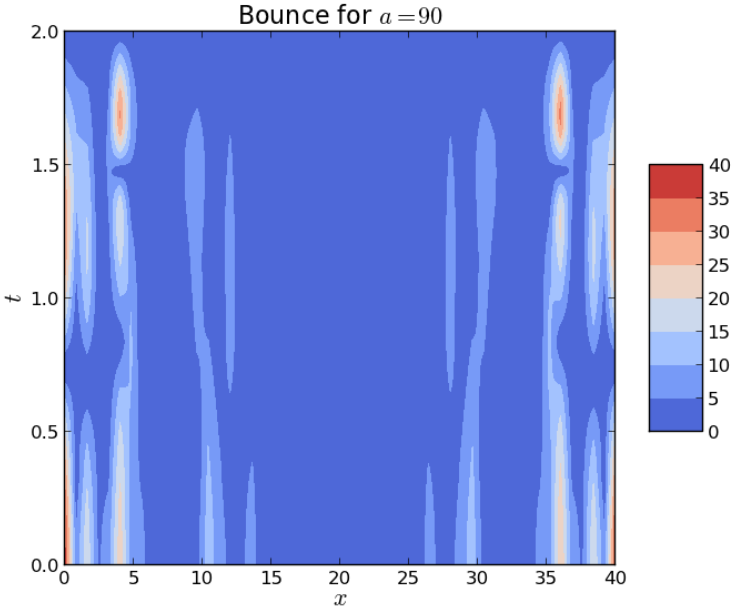

FIGURE 6.11: The Minkowski extension of the bounce for a=0.90 showing divergence after 6 steps

In this section the first numerical results are found which give confidence in the use of the numerical algorithm on the lattice. This is required for the more complicated non-real solutions and periodic instantons extended into Minkowski space. The Hamiltonian was found to be conserved within expected bounds and the results for the bounce agreed with those found by Mathematica to high precision. An investigation of the thin wall limit showed that $a > 0.97$ for this to give accurate results but that the general exponential dependence is exhibited. The continuation into the Minkowski regime was begun, however, more work is required here.

Chapter 7

Conclusions

The main aim of this report was to show how to derive the semi-classical approximations for first the spontaneous vacuum decay and then the phenomenologically interesting case of induced vacuum decay. These results were then transformed into a form that could be solved numerically on a lattice. Initial results were found with which the form of the bounce for QM and QFT for a sample potential were found. These were used to calculate the suppression exponent for the spontaneous decay of the metastable state. Throughout this analysis the results were checked such that energy conservation was satisfied and the bounce action agreed with the solution found by Mathematica. The bounce action gives the suppression to the decay of the metastable state and this was found as expected to increase with barrier height. The continuation of the solution into the Minkowski region was begun. This lattice simulation is a relatively new technique and therefore it is good to see that it can be applied in these simple cases. The next step must be to continue further into the Minkowski region to observe the expanding bubble behaviour. After this the more complicated case of induced vacuum decay may be simulated. With more time a larger and therefore more accurate lattice would be used which should also avoid interference from the boundaries on the bounce. It would also be of much interest to look at other cases of bubble nucleation such as that driven by magnetic monopoles [32]. With more time a greater depth of analysis of the solutions found would also have been desired. This area is quite unique in that it is important for any theory that may contain false scalar vacuums. Recently the has been a lot of interest in such vacua in String Theory and Supersymmetry [33], [34]. The value of the work described in this report is that it can easily be extended to such theories.

Acknowledgements

Many thanks to Arttu Rajantie for all of his help and advice, especially in the numerical implementation section of the project. Thanks also to Simon Nakach and Nick Poovuttikul for their help with LaTeX and Mathematica.

Appendix A

Coherent State Formalism

A.1 Harmonic Oscillator

First consider the harmonic oscillator in 1D quantum mechanics. The Hamiltonian is given by

$$\bar{H} = \frac{\bar{p}^2}{2m} + \frac{1}{2}m\omega^2\bar{q}^2 \tag{A.1}$$

where $\bar{p}$ and $\bar{q}$ are the momentum and position operators respectively and ω is the frequency of the oscillator. A state excited to level n is defined by

$$|n\rangle = \frac{a^\dagger}{\sqrt{n!}}|0\rangle$$

where a is the annihilation operator. Consider now the state $|a\rangle$ defined by:

$$\hat{a}|a\rangle = a|a\rangle. \tag{A.2}$$

Such a state is known as a coherent state. In the coordinate representation this may be written as

$$\langle q|a\rangle = N.exp(-\frac{1}{2}a^2 - \frac{1}{2}\frac{\omega}{q^2} + \sqrt{2\omega}aq). \tag{A.3}$$

The coherent state representation of $|n\rangle$ is given by

$$\psi_n(a^*) \equiv \langle a|n\rangle = \langle a|0\rangle\frac{(a^*)^n}{\sqrt{n!}} \tag{A.4}$$

and to determine the constant $\langle a|0\rangle$ consider

$$1 = \sum_n \langle a|n\rangle\langle n|a\rangle = |\langle 0|a\rangle|^2 \mathrm{e}^{|a|^2} \tag{A.5}$$

giving the normalisation

$$\langle a|0\rangle = \mathrm{e}^{-1/2|a|^2}. \tag{A.6}$$

Normalising such that

$$\psi_n(a^*) \equiv \langle a|n\rangle = \frac{(a^*)^n}{\sqrt{n!}}, \tag{A.7}$$

the completeness relation is then written as

$$\int \frac{\mathrm{d}^2 a}{\pi} \mathrm{e}^{-|a|^2} |a\rangle\langle a| = 1 \tag{A.8}$$

where

$$a = r\mathrm{e}^{i\theta} \rightarrow \mathrm{d}^2 a = r dr d\theta \tag{A.9}$$

and the scalar product between states is written

$$\langle \psi_n|\psi_m\rangle = \int \mathrm{e}^{-|a|^2} \frac{\mathrm{d}^2 a}{\pi} [\psi_n(a^*)]^* \psi_m(a^*). \tag{A.10}$$

Operators are defined by their kernel $A(b^*, a) \equiv \langle b|\hat{A}|a\rangle$ and act as

$$(\hat{A}\psi)(b^*) = \int \mathrm{e}^{-|a|^2} \frac{\mathrm{d}^2 a}{\pi} A(b^*, a)\psi(a^*). \tag{A.11}$$

Finally the overlap between two coherent states is given by:

$$\langle a|b\rangle = \sum_n \langle a|n\rangle\langle n|b\rangle = \sum_n \frac{a^* b^n}{n!} = \mathrm{e}^{a^* b}. \tag{A.12}$$

A.2 Scalar Field Theory

These results may be translated to field theory where the states are eigenstates of the annihilation operator of momentum k, $\hat{a}_k$

$$\hat{a}_k|\{a_k\}\rangle = a_k|\{a_k\}\rangle \forall k \tag{A.13}$$

The starting point for Chapter 4 is the generalisation of A.3 to scalar field theory which gives

$$\langle \phi|\{a_k\}\rangle = N.exp\left[-\frac{1}{2}\int \mathrm{d}k a_k a_{-k} - \frac{1}{2}\int \mathrm{d}k \omega_k \tilde{\phi}(k)\tilde{\phi}(-k) + \int \mathrm{d}k \sqrt{2\omega_k} a_k \tilde{\phi}(k)\right] \tag{A.14}$$

where

$$\frac{1}{(2\pi)^{3/2}} \int \mathrm{d}x e^{ik.x} \phi(x) \equiv \tilde{\phi}(k) \tag{A.15}$$

is the spatial Fourier transform of $/phi(x)$. Equations A.8, A.10 and A.11 are generalised similarly.

Appendix B

Saddle Point Method

This derivation follows [12]. Consider an integral of the form

$$I(N) = \int_a^b \mathrm{d}z g(z) \mathrm{e}^{Nf(z)} \quad N \gg 0 \tag{B.1}$$

where $f(z)$ is a complex analytic function and N is a real number. Define $f(z) = u + iv$, the integral will be dominated by values of u near its maximum. On the other hand if v is not stationary then the oscillating contributions will cancel. This implies the largest contribution will be for $f'(z) = 0$. This must be a saddle point of $f(z)$. In the case of several saddle points the integral is dominated by the highest. Assuming this is at z_0 by Cauchy's integral theorem the contour may be deformed such that it goes through that point. Near z_0 $g(z) \simeq g(z_0)$ and $f(z)$ can be written as

$$f(z) \simeq f(z_0) + \frac{1}{2} f''(z_0)(z - z_0). \tag{B.2}$$

The integral then becomes

$$I(N) \simeq g(z_0) \mathrm{e}^{Nf(z_0)} \oint_C \mathrm{d}z exp\left[\frac{1}{2} N f''(z_0)(z - z_0)^2\right]. \tag{B.3}$$

Using a change of variables as

$$z - z_0 = r\mathrm{e}^{i\phi} \quad f''(z_0) = |f''(z_0)|\mathrm{e}^{i\theta}$$

The choice of ϕ will not affect the result as this only controls the approach angle of the contour to the saddle point. By choosing it as $\phi = (\pi - \theta)/2$ the integral simplifies to

$$I(N) \simeq g(z_0) \mathrm{e}^{Nf(z_0)} \mathrm{i}\phi \int \mathrm{d}r exp\left[-\frac{1}{2} N |f''(z_0)\ vertr^2\right] \tag{B.4}$$

This is now just a Gaussian integral and the result is

$$I(N) \simeq g(z_0)\mathrm{e}^{Nf(z_0)}\mathrm{i}\phi\frac{2\pi}{|Nf''(z_0)|}^{2}. \tag{B.5}$$

This is the saddle point approximation to the integral. It is also known as the method of steepest descent. This is because this choice of ϕ corresponds to a path of steepest descent from the saddle point.

Appendix C

Symmetric Double Well

C.1 Symmetric Double Well

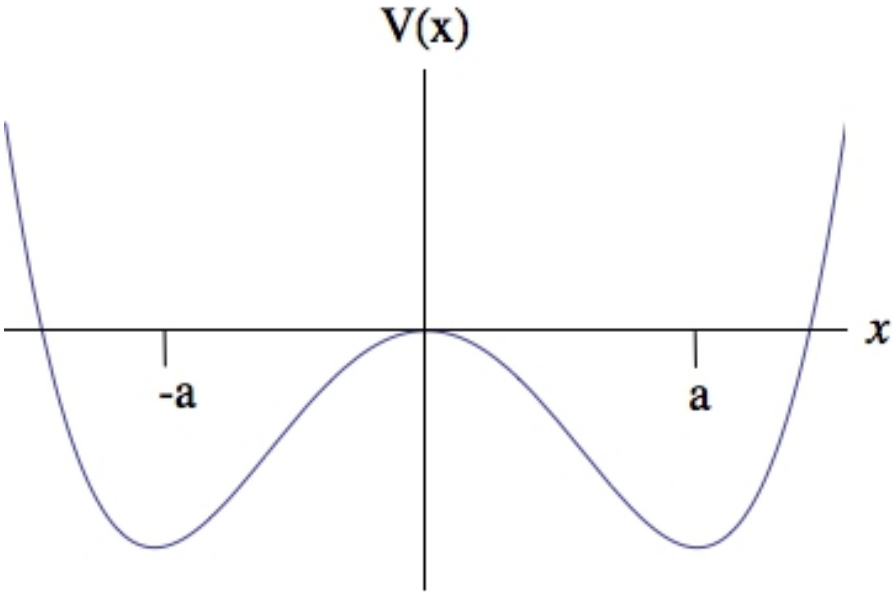

FIGURE C.1: The symmetric double well has a degeneracy in the minima, complicating the solution

The derivation for a symmetric double well follows exactly that for the case of false minimum decay up to 2.43. Consider figure C.1. By symmetry it is possible to start and end an instanton path in either $x = \pm a$. For false vacuum decay there is no degeneracy between the minima and so an instanton path had to start and end at $x = 0$. Now, however, this is no longer the case and so an instanton is taken to refer to a path which starts at $x = -a$ and ends at $x = +a$ while an anti-instanton refers to the opposite path. By symmetry both give the same contribution and will be referred to as bounces (K is implicitly redefined to account for this). However, there will be a difference in the

case which ends at the opposite minimum to that which does not as $\tau_0 \to \infty$. In the first case there will be an odd number of bounces and in the second an even number. Therefore the sum for each case will be over odd and even numbers of pseudo particles respectively.

$$\langle \pm a|\mathrm{e}^{-H\tau_0}|a\rangle = \sum_{neven/nodd}^{\infty} \left(\frac{\omega}{\pi}\right)^{1/2} \mathrm{e}^{-\omega\tau_0/2} \frac{\left(K\mathrm{e}^{-S_0}\right)}{n!} = \left(\frac{\omega}{\pi}\right)^{1/2} \mathrm{e}^{-\omega\tau_0/2} \frac{1}{2} \left[exp(K\mathrm{e}^{-S_0}T) \pm exp(-K\mathrm{e}^{-S_0}T)\right. \tag{C.1}$$

Therefore there are now two eigenstates with energies

$$E_{\pm} = \frac{1}{2}\omega \pm K\mathrm{e}^{-S_0} \tag{C.2}$$

Denoting these eigenstates by $|+\rangle$ and $|-\rangle$ the expectation values may also be read

$$|\langle +| \pm a\rangle|^2 = |\langle -| \pm a\rangle|^2 = -\langle a|-\rangle\langle -| - a\rangle = -\langle a|+\rangle\langle +| - a\rangle = \frac{1}{2}\left(\frac{\omega}{\pi}\right)^{1/2} \tag{C.3}$$

and so there is not a degeneracy in the particle position but instead it can exist in either well with the effect of tunnelling "smearing" the ground states. The lowest energy state will be that with an even superposition of the wavefunctions in each well while the higher energy corresponds to an odd superposition. The shift of the energy in C.2 is actually much smaller than neglected terms due to the exponential suppression. It is included, however, as this is the highest order term in the energy difference between these two states. It is shown in [15] that this gives the correct result for the potential $V = \lambda(x^2 - \eta^2)^2$.

Bibliography

[1] A.D. Linde. Scalar field fluctuations in the expanding universe and the new inflationary universe scenario. *Physics Letters B*, 116(5):335 – 339, 1982. ISSN 0370-2693. doi: http://dx.doi.org/10.1016/0370-2693(82)90293-3. URL http://www.sciencedirect.com/science/article/pii/0370269382902933.

[2] G. S. Guralnik, C. R. Hagen, and T. W. B. Kibble. Global conservation laws and massless particles. *Phys. Rev. Lett.*, 13:585–587, Nov 1964. doi: 10.1103/PhysRevLett.13.585. URL http://link.aps.org/doi/10.1103/PhysRevLett.13.585.

[3] Gino Isidori, Vyacheslav S. Rychkov, Alessandro Strumia, and Nikolaos Tetradis. Gravitational corrections to standard model vacuum decay. *Phys. Rev. D*, 77: 025034, Jan 2008. doi: 10.1103/PhysRevD.77.025034. URL http://link.aps.org/doi/10.1103/PhysRevD.77.025034.

[4] *Soviet Journal of Nuclear Physics*, 20:644, 1974.

[5] Sidney Coleman. Fate of the false vacuum: Semiclassical theory. *Phys. Rev. D*, 15: 2929–2936, May 1977. doi: 10.1103/PhysRevD.15.2929. URL http://link.aps.org/doi/10.1103/PhysRevD.15.2929.

[6] Sidney. Coleman. Cambridge University Press, 1985. URL http://dx.doi.org/10.1017/CBO9780511565045.

[7] Andrei Linde. Hybrid inflation. *Phys. Rev. D*, 49:748–754, Jan 1994. doi: 10.1103/PhysRevD.49.748. URL http://link.aps.org/doi/10.1103/PhysRevD.49.748.

[8] Minoru Eto, Yuta Hamada, Kohei Kamada, Tatsuo Kobayashi, Keisuke Ohashi, and Yutaka Ookouchi. Cosmic r-string, r-tube and vacuum instability. *Journal of High Energy Physics*, 2013(3):1–25, 2013. doi: 10.1007/JHEP03(2013)159. URL http://dx.doi.org/10.1007/JHEP03%282013%29159.

[9] S. V. Demidov and D. G. Levkov. Soliton-antisoliton pair production in particle collisions. *Phys. Rev. Lett.*, 107:071601, Aug 2011. doi: 10.1103/PhysRevLett.107.071601. URL http://link.aps.org/doi/10.1103/PhysRevLett.107.071601.

[10] Curtis G. Callan and Sidney Coleman. Fate of the false vacuum. ii. first quantum corrections. *Phys. Rev. D*, 16:1762–1768, Sep 1977. doi: 10.1103/PhysRevD.16.1762. URL http://link.aps.org/doi/10.1103/PhysRevD.16.1762.

[11] Mikhail A. Shifman. ITEP lectures on particle physics and field theory. Vol. 1, 2. *World Sci.Lect.Notes Phys.*, 62:1–875, 1999.

[12] Davide Marenduzzo. Methods of Mathematical Physics Lecture 5. *http://www2.ph.ed.ac.uk/ dmarendu/MOMP/lecture05.pdf*.

[13] E. C. G. Sudarshan, C. B. Chiu, and Vittorio Gorini. Decaying states as complex energy eigenvectors in generalized quantum mechanics. *Phys. Rev. D*, 18:2914–2929, Oct 1978. doi: 10.1103/PhysRevD.18.2914. URL http://link.aps.org/doi/10.1103/PhysRevD.18.2914.

[14] A.A. Belavin and A.M. Polyakov. Quantum fluctuations of pseudoparticles. *Nuclear Physics B*, 123(3):429 – 444, 1977. ISSN 0550-3213. doi: http://dx.doi.org/10.1016/0550-3213(77)90175-4. URL http://www.sciencedirect.com/science/article/pii/0550321377901754.

[15] Marcos Marino. Instantons and large n. *Lecture Notes, http://www. cuso*, 2009.

[16] A Pankov. Introduction to Spectral Theory of Schrödinger Operators. *http://www.math.nsysu.edu.tw/ amen/posters/pankov.pdf*.

[17] Sidney Coleman, Vladimir Glaser, and Andre Martin. Action minima among solutions to a class of euclidean scalar field equations. *Communications in Mathematical Physics*, 58(2):211–221, 1978.

[18] Raphael Bousso, Daniel Harlow, and Leonardo Senatore. Inflation after False Vacuum Decay: Observational Prospects after Planck. 2013.

[19] S.Yu. Khlebnikov, V.A. Rubakov, and P.G. Tinyakov. Periodic instantons and scattering amplitudes. *Nuclear Physics B*, 367(2):334 – 358, 1991. ISSN 0550-3213. doi: http://dx.doi.org/10.1016/0550-3213(91)90020-X. URL http://www.sciencedirect.com/science/article/pii/055032139190020X.

[20] V.A. Rubakov and P.G. Tinyakov. Towards the semiclassical calculability of high energy instanton cross sections. *Physics Letters B*, 279(1–2):165 – 168, 1992. ISSN 0370-2693. doi: http://dx.doi.org/10.1016/0370-2693(92)91859-8. URL http://www.sciencedirect.com/science/article/pii/0370269392918598.

[21] P.G. Tinyakov. Multiparticle instanton-induced processes. application to b violation in high energy collisions. *Physics Letters B*, 284(3–4):410 – 416, 1992. ISSN 0370-2693. doi: http://dx.doi.org/10.1016/0370-2693(92)90453-B. URL http://www.sciencedirect.com/science/article/pii/037026939290453B.

[22] Claudio Rebbi and Jr Singleton, Robert L. Numerical approaches to high-energy electroweak baryon number violation above and below the sphaleron barrier. 1996.

[23] Haim Goldberg. Breakdown of perturbation theory at tree level in theories with scalars. *Phys.Lett.*, B246:445–450, 1990. doi: 10.1016/0370-2693(90)90628-J.

[24] Alexander Kyatkin. Multiparticle semiclassical process in phi**4 theory. *Phys.Lett.*, B316:318–323, 1993. doi: 10.1016/0370-2693(93)90331-B.

[25] S.Yu. Khlebnikov, V.A. Rubakov, and P.G. Tinyakov. Instanton induced cross sections below the sphaleron. *Nuclear Physics B*, 350(1–2):441 – 473, 1991. ISSN 0550-3213. doi: http://dx.doi.org/10.1016/0550-3213(91)90267-2. URL http://www.sciencedirect.com/science/article/pii/0550321391902672.

[26] V.A. Rubakov, D.T. Son, and P.G. Tinyakov. An Example of semiclassical instanton like scattering: (1+1)-dimensional sigma model. *Nucl.Phys.*, B404:65–90, 1993. doi: 10.1016/0550-3213(93)90473-3.

[27] D.G. Levkov and S.M. Sibiryakov. Induced tunneling in QFT: Soliton creation in collisions of highly energetic particles. *Phys.Rev.*, D71:025001, 2005. doi: 10.1103/PhysRevD.71.025001.

[28] F.L. Bezrukov, D. Levkov, C. Rebbi, V.A. Rubakov, and P. Tinyakov. Semiclassical study of baryon and lepton number violation in high-energy electroweak collisions. *Phys.Rev.*, D68:036005, 2003. doi: 10.1103/PhysRevD.68.036005.

[29] A. N. Kuznetsov and P. G. Tinyakov. False vacuum decay induced by particle collisions. *Phys. Rev. D*, 56:1156–1169, Jul 1997. doi: 10.1103/PhysRevD.56.1156. URL http://link.aps.org/doi/10.1103/PhysRevD.56.1156.

[30] D. Levkov and S. Sibiryakov. Real-time instantons and suppression of collision-induced tunneling. *Journal of Experimental and Theoretical Physics Letters*, 81(2): 53–57, 2005. ISSN 0021-3640. doi: 10.1134/1.1887914. URL http://dx.doi.org/10.1134/1.1887914.

[31] Physics 212: Statistical mechanics ii lecture xvi. October 2010. doi: Accessedon01/09/13. URL http://socrates.berkeley.edu/~jemoore/Moore_group,_UC_Berkeley/Physics_212_files/phys212ln16.pdf.

[32] Brijesh Kumar, M. B. Paranjape, and U. A. Yajnik. Fate of the false monopoles: Induced vacuum decay. *Phys. Rev. D*, 82:025022, Jul 2010. doi: 10.1103/PhysRevD.82.025022. URL http://link.aps.org/doi/10.1103/PhysRevD.82.025022.

[33] Alexander Kusenko. Supersymmetry in the false vacuum. *Physics Letters B*, 377(4):245 – 249, 1996. ISSN 0370-2693. doi: http://dx.doi.org/10.1016/0370-2693(96)00405-4. URL http://www.sciencedirect.com/science/article/pii/0370269396004054.

[34] Borut Bajc, Gia Dvali, and Goran Senjanovic. Problems with False Vacua in Supersymmetric Theories. 2011.